

BRITISH GEOLOGICAL SURVEY

Fluid Processes and Waste Management Group

TECHNICAL REPORT WE/98/38

**Electrokinetic Sounding Results,
INCO-DC Project 950176,
Israel, 1998**

David Beamish

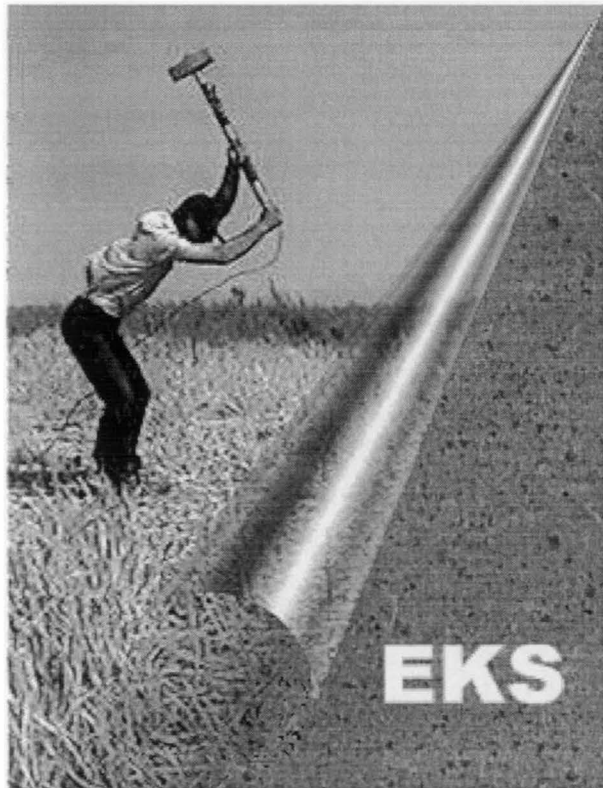
Bibliographic Reference :

Beamish D., 1998.

***Electrokinetic Sounding Results,
INCO-DC Project 950176,
Israel, 1997.***

*British Geological Survey,
Technical Report, WE/98/38*

A report prepared for:
European Commission
DG-XII
Directorate B
Programme INCO-DC
75, Rue Montoyer
B-1040 Brussels



British Geological Survey, Keyworth, Nottingham, 1998

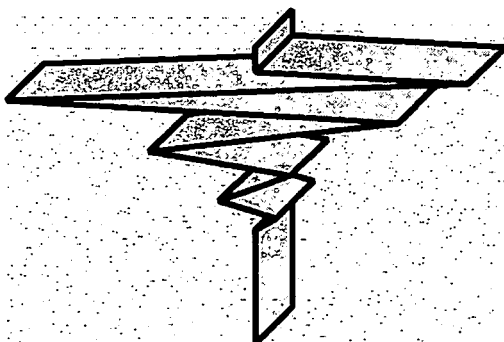
©NERC copyright 1998



This report has been generated from a scanned image of the document with any blank pages removed at the scanning stage.
Please be aware that the pagination and scales of diagrams or maps in the resulting report may not appear as in the original

CONTENTS

1) Introduction	2
2) EK Survey	2
3) Comparison of seismic sources	4
3.1) Comparison at site B	4
3.2) Comparison at site E	5
4) Moveout effects	5
5) EK results	6
6) Hydrogeological estimates	6
7) Summary	7
8) References	8
9) Acknowledgements	8



1) Introduction

This report summarises the results of work undertaken for the EEC INCO-DC project: A new integrated geophysical approach for the rational management and exploration of groundwater resources. The programme Project Number is 950176 under Contract Number ERBIC 18 CT 960122.

EU member participants are:

The Netherlands:	RGD: (NITG-TNO), Haarlem James Baker (Project Coordinator)	
France:	BRGM, Orleans Alain Beauce	
U.K.:	BGS, Nottingham D. Beamish and Jon Busby	

Non-EU partners are:

Cyprus:	GSD, Nicosia Sortiris Kramvis	GEOINVEST, Nicosia Andreas Shiathas
Israel:	GII, Holon Mark Goldman	

Two previous reports summarised the field activities of the Electrokinetic Sounding (EKS) technique which took place on Cyprus during June 1997 (Beamish, 1997) and May/June 1998 (Beamish, 1998). This report summarises an EKS survey which took place in Israel during February 1998. The survey location map of the Nitzanim area is shown in Figure 1.1.

2) EK Survey

A total of nine EK soundings were made along the main geophysical traverse line at Nitzanim as shown in Figure 2.1. The soundings are denoted by letters from A to I with increasing distance from the coast. Over the total length of the EK survey (coast in the west to 1126 m inland) additional control is provided by:

- 1) 3 deep hydrogeological control boreholes: BH12/0, BH12/B and BH12/A.
- 2) 4 TEM soundings: NIZ_1, NIZ_2, NIZ_3 and NIZ_4.
- 3) 5 PMR soundings

Water table depths in the boreholes are estimated to be within 1 m of the elevations given in Table 1 (below).

The majority of this control is located between boreholes 12/0 and 12/A (Fig. 2.1). The EK survey was extended further inland towards seismic line GI-0083.

Using the coast as origin, the EK soundings have profile coordinates shown in Table 1.

Site	Distance (m)	Elevation (m)	Seismic source	Comments	Field code
A	100.0	8.5	Hammer	Next to BH12/0	1/F04
B	100.0	8.5	Hammer + Dyna	On track next to BH12/0	1A/F04
C	573.0	16.0	Hammer + Dyna	Close to BH12/B	2/F04
D	741.0	20.0	Hammer	On track between boreholes	6/F05
E	867.0	30.0	Hammer + Dyna	Topo high above BH12/A	3/F04
F	950.0	19.8	Hammer	Next to BH12/A	5/F05
G	1010.0	16.0	Hammer + Dyna	Topo low, below main N-S track	4/F05
H	1076.0	31.0	Hammer	Above main N-S track	8/F05
I	1126.0	46.0	Hammer	Just below location of GI-0083	7/F05

At four locations, conventional EK hammer soundings were repeated using the truck-mounted Dynasource system (truck mounted vacuum accelerated weightdrop) provided by GII. Pictures of field operations using the two sources are shown in Figure 2.2.

The standard EK sounding configuration used on the survey comprised a linear, shot-symmetric 8-channel array of 2 m dipoles. On each side of the shot, 2 m dipoles were deployed from 0.5 to 2.5 m, 1.0 to 3.0 m, 2.0 to 4.0 m and from 5.0 to 7.0 m. The first electrode pair is referred to as the inner electrode pair and typically records the largest amplitude signals. The additional electrode pairs are used to examine the moveout behaviour of the recorded signals. The outer electrode pair (5 to 7 m) proved largely ineffective (in terms of signal/noise) due to the rapid spatial decay of the signals from the source location.

The near-surface environment comprised wind-blown sand dunes with occasional loam as shown in Figure 2.3. The EK methodology requires that the stainless steel electrodes making up the dipoles be inserted rigidly into the ground. This is clearly difficult in loose sand (see Figure 2.3) causing poor data quality from some dipoles. This problem was further exacerbated when the larger energy Dynasource source was used. Following electrode deployment the same array was used for both hammer and Dynasource recordings.

Contact resistances, following watering of the electrodes, were typically 5 to 10 kohm. In some cases individual dipole resistances were in excess of 1 Megohm. Data quality varied across the survey. The sounding with by far the best overall data quality was sounding D

which was made along the site access track. At this location the mixture of sand and loam provided much better rigidity and electrical contact (typically 600 to 800 ohm).

3. Comparison of seismic sources.

A comparison of the data obtained using the conventional hammer source and the GII Dynasource at sites B and E now follows.

3.1 Comparison at site B.

Dynasource recordings made at site B are now considered. The inner 2 channels (± 0.5 to 2.5 m) are used for illustration. Figure 3.1 (a,b) shows the voltage data obtained from a sequence of shots (21 to 24) from the inner 2 channels. The entire recording (400 ms) is shown in the upper frame and the initial 60 ms are shown, in detail, in the lower frame.

The two data channels are entirely in-phase and the response is dominated by a large negative excursion (> 15 mV/m) within the first 20 ms. The relatively high frequency oscillation then decays slowly to zero by about 150 ms. Shots 21, 22 and 23 provide a second (source-related) large amplitude pulse at times > 150 ms. The pulse is in-phase on the two channels. To demonstrate the time-variability of the effect, shot 24 provides a different form of pulse centered on 50 ms. Again the oscillation is in-phase. These interspersed later time effects are taken to be complex, partially repeatable source-related effects such as double-bounce.

During later Dynasource shots at site B, a further source-related effect was observed. Figure 3.2 shows three successive shots (35 to 37) in which a form of 'second sounding' is initiated (presumably by a second 'clean' strike of the source-plate) between 150 and 200 ms.

For comparison, 3 successive hammer shots from sounding site B are shown in Figure 3.3. Clearly the voltage response observed using the hammer is an order of magnitude less than that obtained using the high-energy Dynasource. It is also apparent that the much lower amplitude data characteristics, particularly across the first 10 ms, display a different character. Between 10 and 20 ms there is an important similarity between Figures 3.1b and 3.3; a point of inflection occurs which appears to be associated with the termination of the initial (early-time) oscillations. Following the inflection, between 15 and 30 ms, the two channels are 'separated' before becoming together at a positive voltage and slowly decaying together (in-phase) with increasing time.

Selected shot records were used to provide stacked results for the two sources. The two-channel results for the first 60 ms are shown in Figure 3.4a (hammer source) and Figure 3.4b (Dynasource). The amplitude scales in Figure 3.4 differ by a factor of 15. The overall consistency of the low frequency, in-phase behaviour is best observed in the trace normalised plots. Apart from the initial behaviour observed in the first few milliseconds, it is clear that the main sounding characteristic is similar for both sources used.

3.2 Comparison at site E.

The sounding at site E is used to further illustrate the voltage recordings obtained using the conventional hammer source and the Dynasource. The inner channels (± 0.5 to 2.5 m) are used in both cases. The data obtained with the hammer source are of particularly poor quality.

Figure 3.5 shows successive shots obtained with the Dynasource at site E at later times. The problem of late-time 'double-bounce' occurred at most sites when the Dynasource was used. In Figure 3.5, a sequence of shots (12-15 and 17) show a similar effect between 180 and 200 ms. Shot 16 (dotted line) shows no effect over the interval shown while the effect for shot 18 slips to later times.

The final stacked soundings using the two sources are shown in Figures 3.6 (hammer source) and 3.7 (Dynasource). The results are shown for the first 60 ms (upper frames) and from 60 to 180 ms (lower frames). In Figure 3.6 (hammer) one of the inner dipoles (single line trace) is not responding 'correctly'. When the hammer source results are compared with the Dynasource results (Figure 3.7), using the same amplitude scales, a general correspondence is apparent. Apart from the fact that one of the hammer dipoles is inconsistent, it is clear that the main sounding characteristic is similar for both sources used.

4. Moveout effects

The standard survey arrangement comprised 2m shot-symmetric dipoles with centres at 1.5 (channels 1&2), 2.0 (channels 3&4), 3.0 (channels 5&6) and 6 m (channels 7&8) from the shot point. This arrangement allows moveout effects to be monitored in detail. The sounding at site D provided the best data quality and is used as an example of the moveout effects repeated at all the survey locations.

Figure 4.1 shows the data obtained across the first 3 channels during the first 30 ms (Fig. 4.1a) and from 60 to 180 ms (Fig. 4.1b). Blue denotes channels 1&2 (channel 2 with infill), red denotes channels 3&4 and black denotes channels 5&6. The voltages recorded by channels 7&8 were at and below the noise level. Data are shown as true amplitudes (left frames) and in trace-normalised form (right frames).

The initial 10 ms of the data is characterised by a positive then negative voltage excursion which is in-phase on all 3 symmetric channels. The amplitude of the oscillation decays rapidly with distance away from the shot point. At an offset (centre dipole) distance of 3 m the maximum oscillation voltage is some 0.25 mV/m. The initial oscillation clearly displays moveout across the array. The moveout behaviour is best examined in the trace-normalised display. The positive/negative excursion has an apparent moveout velocity of between 400 and 440 m/s. The behaviour is consistent with that of surface-wave coupling.

The data obtained at later times (Figure 4.1b) is of much lower amplitude and rapidly decays to < 10 microvolts/m at the larger offsets. Channel 6 is below the noise level however the symmetric channel 5 is well-behaved (i.e. consistent with other channels). The late-time data represent a low-frequency oscillation that is in-phase across the recording array thus indicating valid 'simultaneous' EK coupling vertically beneath the shot point.

5. EK results

The form of display of Figure 4.1 is used to present all the sounding data in a uniform manner. In each case the first 60 ms of the sounding is shown in the upper frames and the time interval from 60 to 180 ms is shown in the lower frames. Both true amplitude and trace-normalised plots are presented. The sounding data for the first two (inner) channels are used since they have the greatest signal/noise. It should be noted that data quality is variable.

Figures 5.1 to 5.4 show the results obtained from soundings A to D away from the coast. Although early time characteristics are variable, consistent behaviour at times > 20 ms is repeated at all four sites. The best data quality is observed at sites C and D.

The sounding obtained with the hammer source at site E (Figure 5.5) was of poor quality so the sounding obtained with the Dynasource is shown in Figure 5.6. Sounding F, made next to BH 12/A is shown in Figure 5.7. Here the sounding is slightly marred by an inconsistent offset between the two channels. The sounding at site G (Figure 5.8) is again of poor quality and the two channels appear inconsistent.

The two soundings (H and I) made furthest from the coast are shown in Figures 5.9 and 5.10, respectively. At these two locations (separated by 50 m) the largest early time voltages were obtained (peak voltages ~ 3 mV/m). The data are of good quality and consistent.

6. Hydrogeological estimates

The estimation of hydrogeological parameters such as porosity and hydraulic permeability from EK sounding data is based on the vertical propagation mode of the acoustic source (Beamish and Peart, 1998; Beamish, 1998). In order to convert time to depth an acoustic velocity model of the subsurface is required. For the Nitzanim survey, velocity estimates are available from the seismic profiles carried out in the area. A 3-layer model consisting of: Layer 1, 0 to 8 m, $V=400$ m/s; Layer 2, 8 to 30 m, $V=1500$ m/s and Layer 3, > 30 m, $V=2000$ m/s, was adopted. Using this model the first interface will be reached in 20 ms. This time interval contains the main positive/negative oscillation, observed at all sites, and interpreted as a surface wave.

The method of analysis estimates interconnected porosity and hydraulic conductivity (permeability) jointly. A number of approximations are involved in the estimation and currently the preferred method of analysis uses normalised, rather than absolute, estimates of the variation of hydraulic conductivity with depth. For a given depth interval, the maximum observed hydraulic conductivity is normalised to unity and all other estimates are relative to this value. For the Nitzanim data, the maximum value is observed invariably in the first 2 metres.

Figures 6.1 to 6.4 show the results obtained for sites A and B (Fig. 6.1), C and D (Fig. 6.2), E and F (Fig. 6.3) and H and I (Fig. 6.4). Sounding G is omitted due to very poor data quality. The result at site E (Fig. 6.3) is shown for the dynasource recording since the hammer source results were of poor quality. All other results shown were obtained with the hammer source. The results shown in Figures 6.1 to 6.4 summarise the estimated hydraulic conductivities to a depth of 60 m. All depths refer to depth below ground surface. The logarithmic scale used for the normalised estimates varies between 2 and 3 decades.

As stated above, the maximum value of conductivity invariably occurs in the first two metres and the deeper variations are now summarised. The main deeper survey characteristic observed is the peak conductivity that occurs at depths between 13 m (site F, Fig. 6.3) and 21 m (site C, Fig. 6.2), discounting the result at site A which is of poor quality. The same 'flat-top' signature to the increase is observed across the 1126 m of the profile making it a 'site-wide', spatially persistent feature. The vertical extent of the zone of enhanced permeability varies slightly in thickness across the profile but generally (ignoring site A) reduces to low values by a depth of 35 mbgl. Significant deeper variations are only found at sites C (Fig. 6.2) and F (Fig. 6.3).

Normalised hydraulic conductivity estimates obtained over the first 10 metres at sites A, B, C, D, E (Dynasource), F, H and I are shown in Figures 6.5 and 6.6. The depth interval shown is prior to the onset of the water table in all cases. The zone is one of partial saturation. At all sites the maximum conductivity is observed in the first two metres of the depth profile. Below this depth, and with the exception of soundings A and F (poor data quality) and sounding E (Dynasource), spatially persistent peaks in hydraulic conductivity are found at depths of 3 and 5 m.

7. Summary

This study probably represents the first use of the EK sounding technique in Israel. The comparison of seismic sources is particularly relevant. It confirms:

- 1) apart from the initial EK signal recorded in the first 10 ms, the same EK sounding characteristics are observed using both high and low energy sources.
- 2) the high energy Dynasource voltage recordings are a factor of 10 to 15 larger than those obtained with the conventional hammer source.

The technical difficulties of using a Dynasource for EK soundings have been investigated and described.

The EK sounding data are of variable quality due to the problems of electrode insertion and high contact resistances in a sand-dune environment. Despite the technical difficulties, valid, in-phase coupling was observed at the majority of sounding locations. The early-time (first 10 ms) coupling displays moveout with a typical velocity of 400 to 440 m/s. A much lower frequency coupling effect is observed at later times. The later-time coupling is observed simultaneously across the recording array. The basic signature the coupling is largely uniform across the survey area.

Estimates of the normalised (relative) hydraulic conductivity as a function of depth have been presented. One-way travel-time has been converted to depth using the same simple, 3-layer acoustic model for all soundings. Hydraulic conductivity is found to maximise in the upper 2 to 2.5 m (below ground level) at all sites. In the shallow subsurface, spatially persistent peaks are found at depths of 3 and 5 m. A second, deeper spatially persistent peak in hydraulic conductivity is found at depths of between 13 m (site F) and 21 m (site C). Significant deeper peaks (i.e. > 25 m) are only found at sites C and F. The accuracy of the depth estimates at individual sites is limited by the accuracy of the 'general' acoustic model adopted for analysis.

8. References

Beamish, D., 1997. Summary of field activities: Year 1, INCO-DC Project 950176, Electrokinetic Sounding. British Geological Survey Technical Report **WE/97/44**. A report prepared for the E.E.C.

Beamish, D., 1998. Electrokinetic sounding results, INCO-DC Project 950176, Cyprus 1997. British Geological Survey Technical Report **WE/98/23**. A report prepared for the E.E.C.

9. Acknowledgements

It is a pleasure to acknowledge the help of all the members of the GII staff who contributed to the field experiment. I would especially like to thank Mark Goldman and Vladimir Shtivelman for arranging all the local logistics and for their generous hospitality.

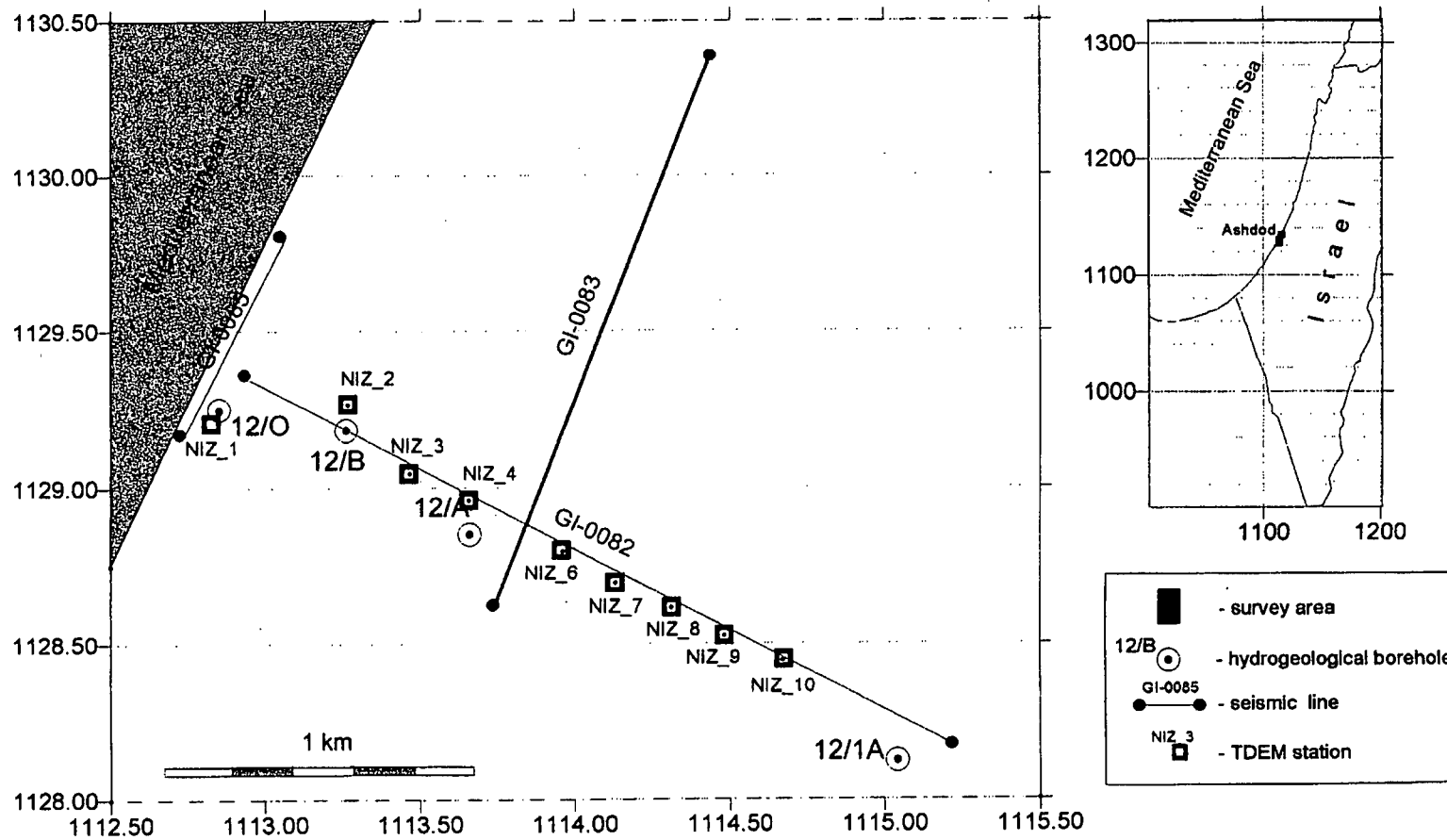


Figure 1.1 Survey location map of the Nitzanim area, showing boreholes, seismic lines and TDEM sounding locations. The EK survey extended from BH 12/0 to seismic line GI-0083

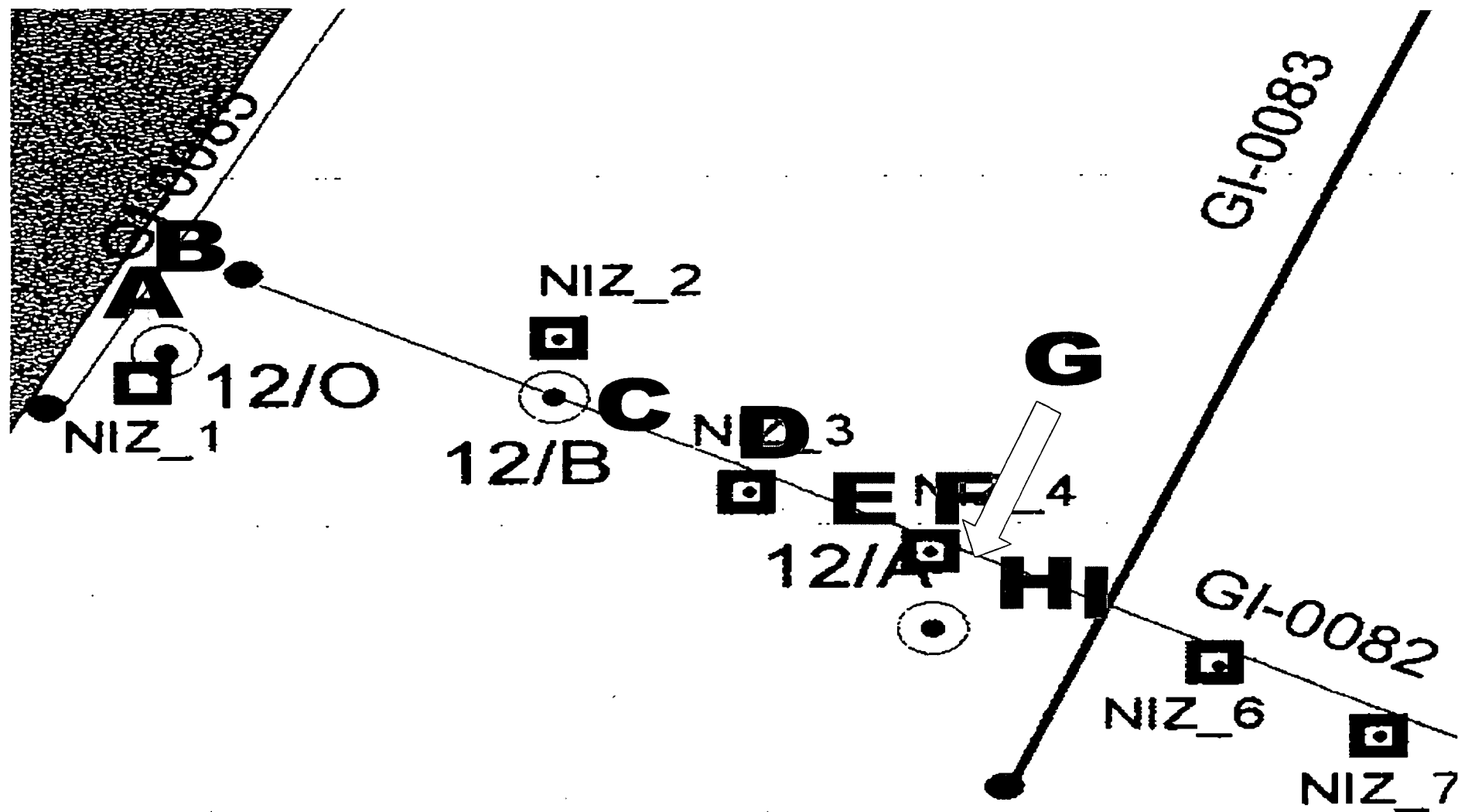
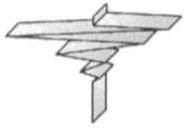


Figure 2.1 EK sounding locations (A to I) along profile GI-0082. Boreholes 12/0, 12/B and 12/A, together with TDEM soundings (square symbols)



Seismic sources

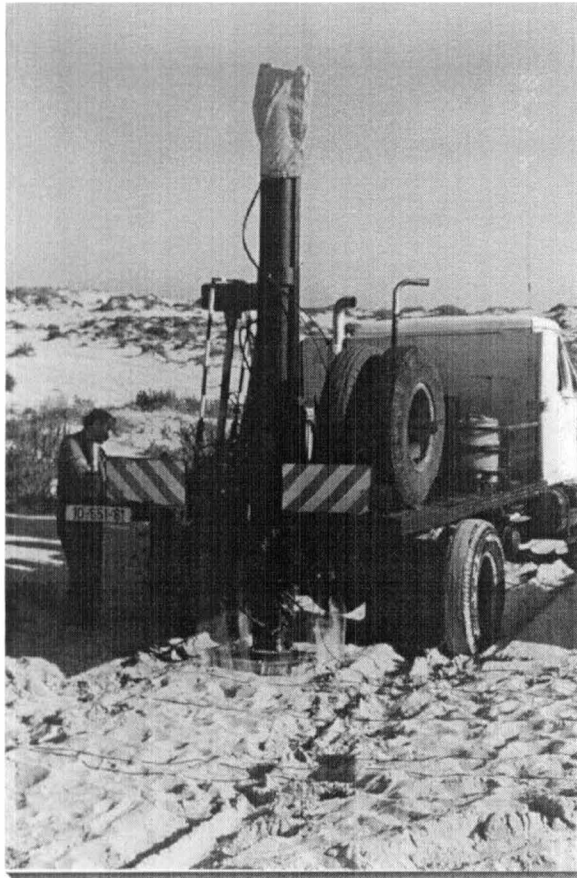
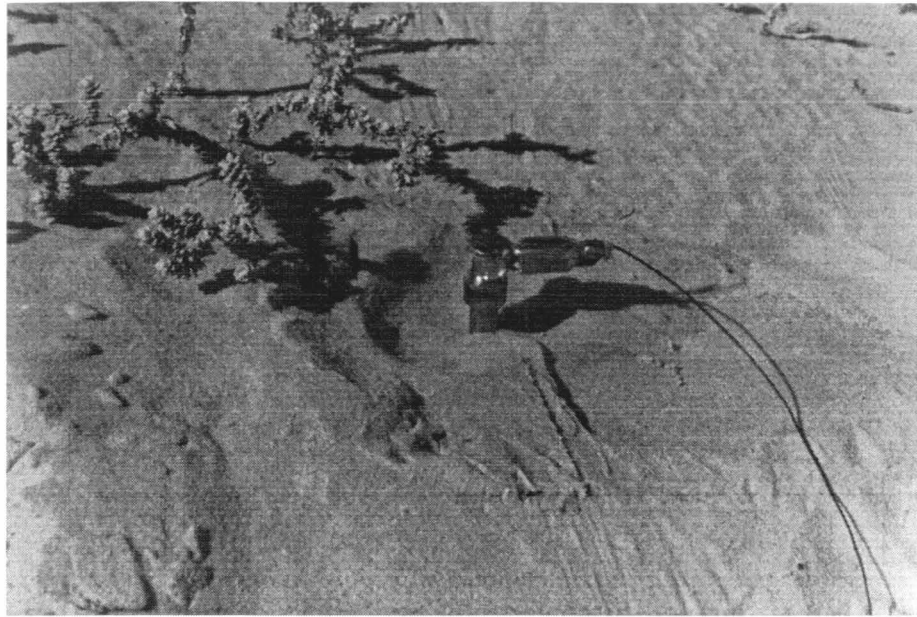


Figure 2.2 Seismic sources used on the Nitzanim survey
Dynasource at site B and hammer at site F

Figure 2.3 Survey ground conditions

a)



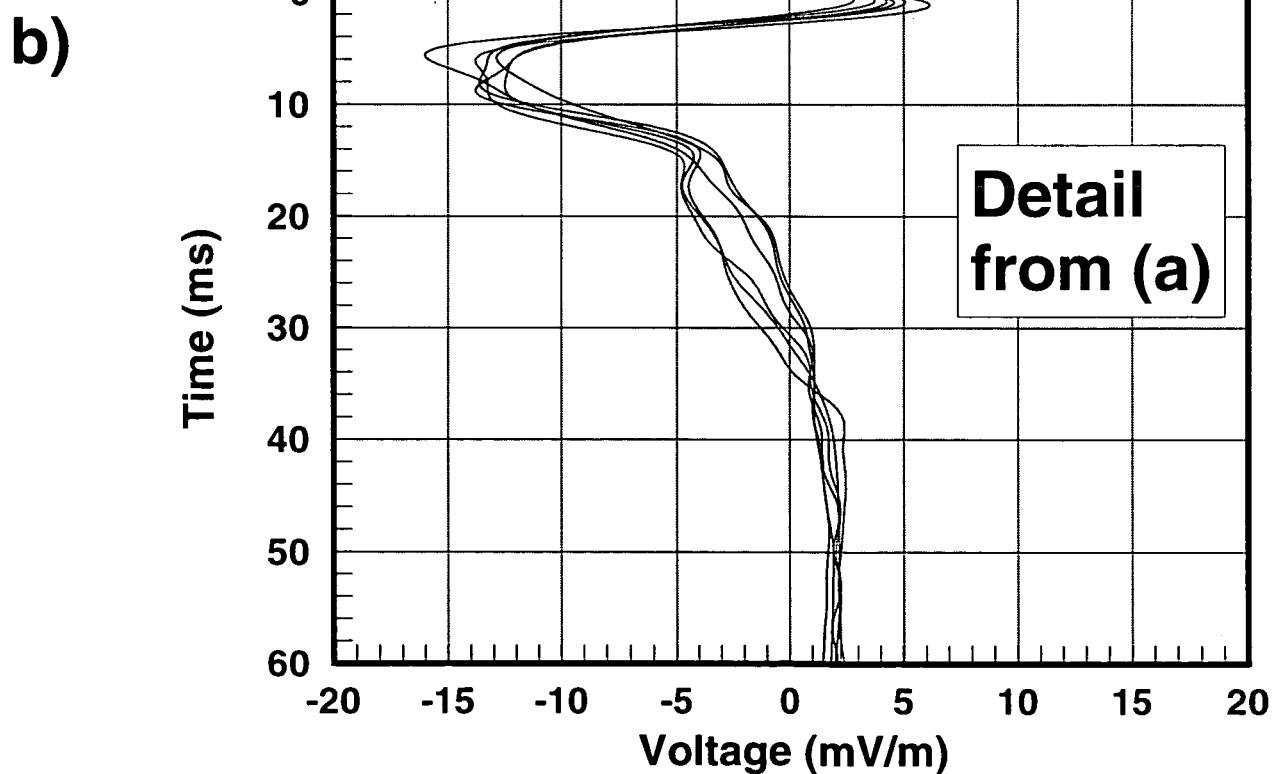
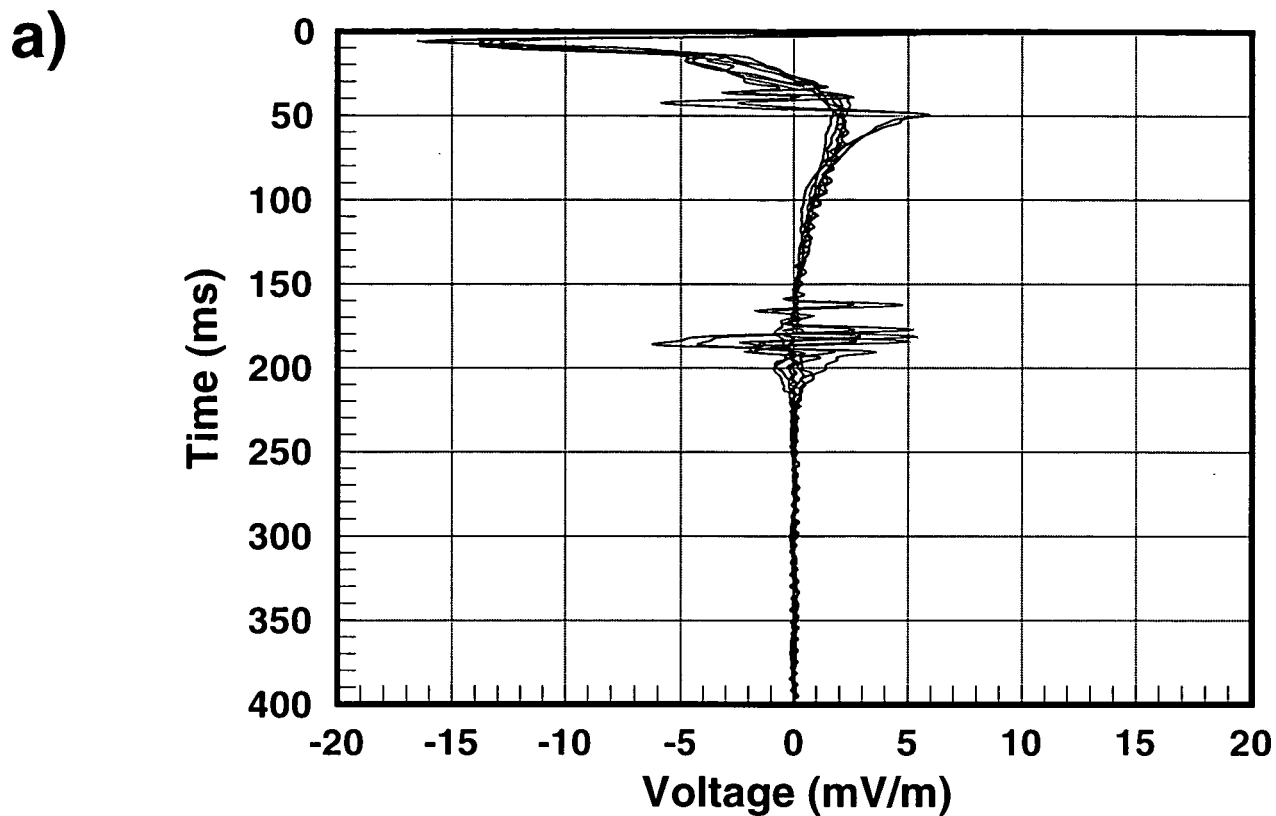
b)



a) Single electrode watered in dry sand

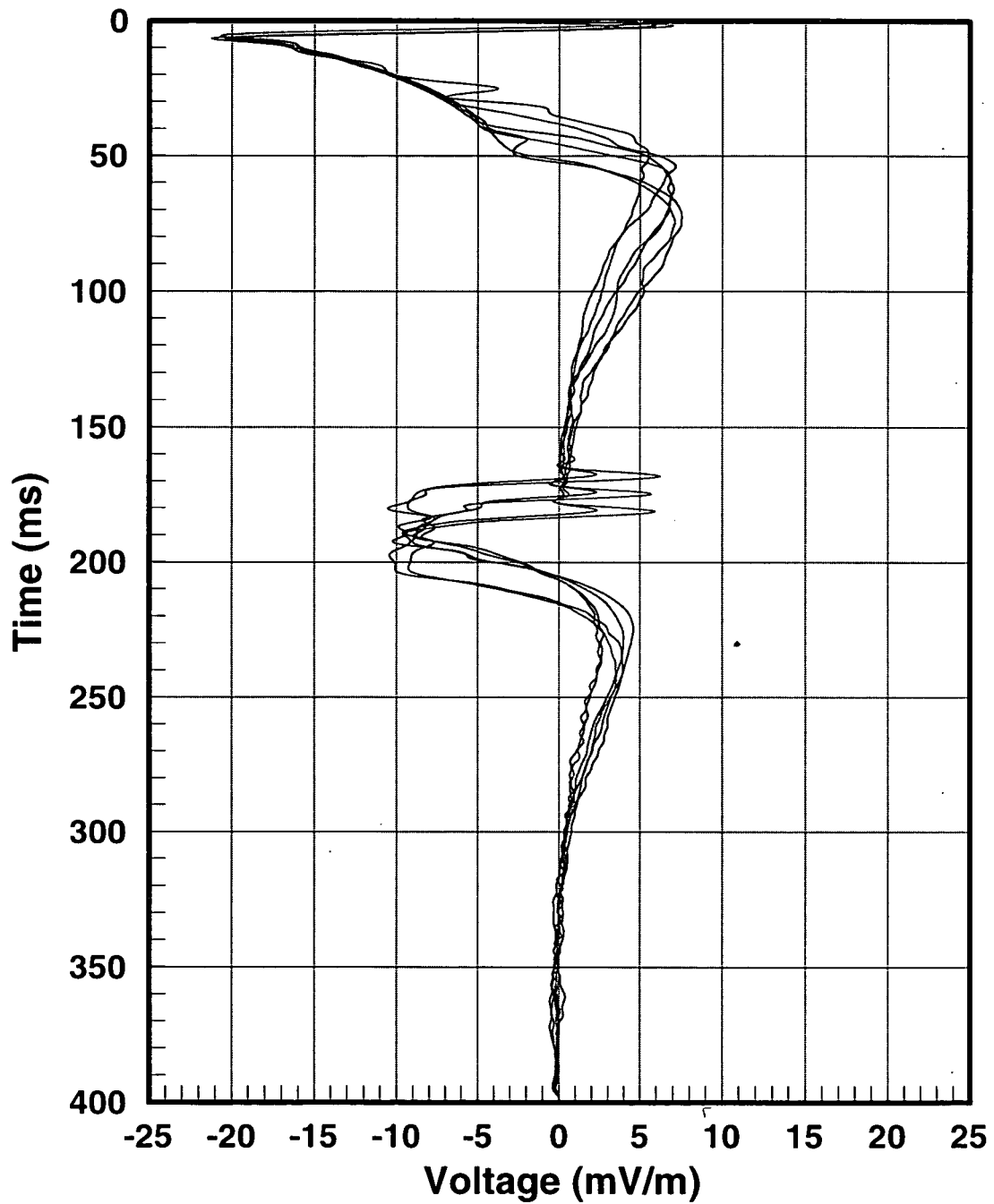
b) plate in pit created by operation of dynasource

Figure 3.1 EK sounding at Site B



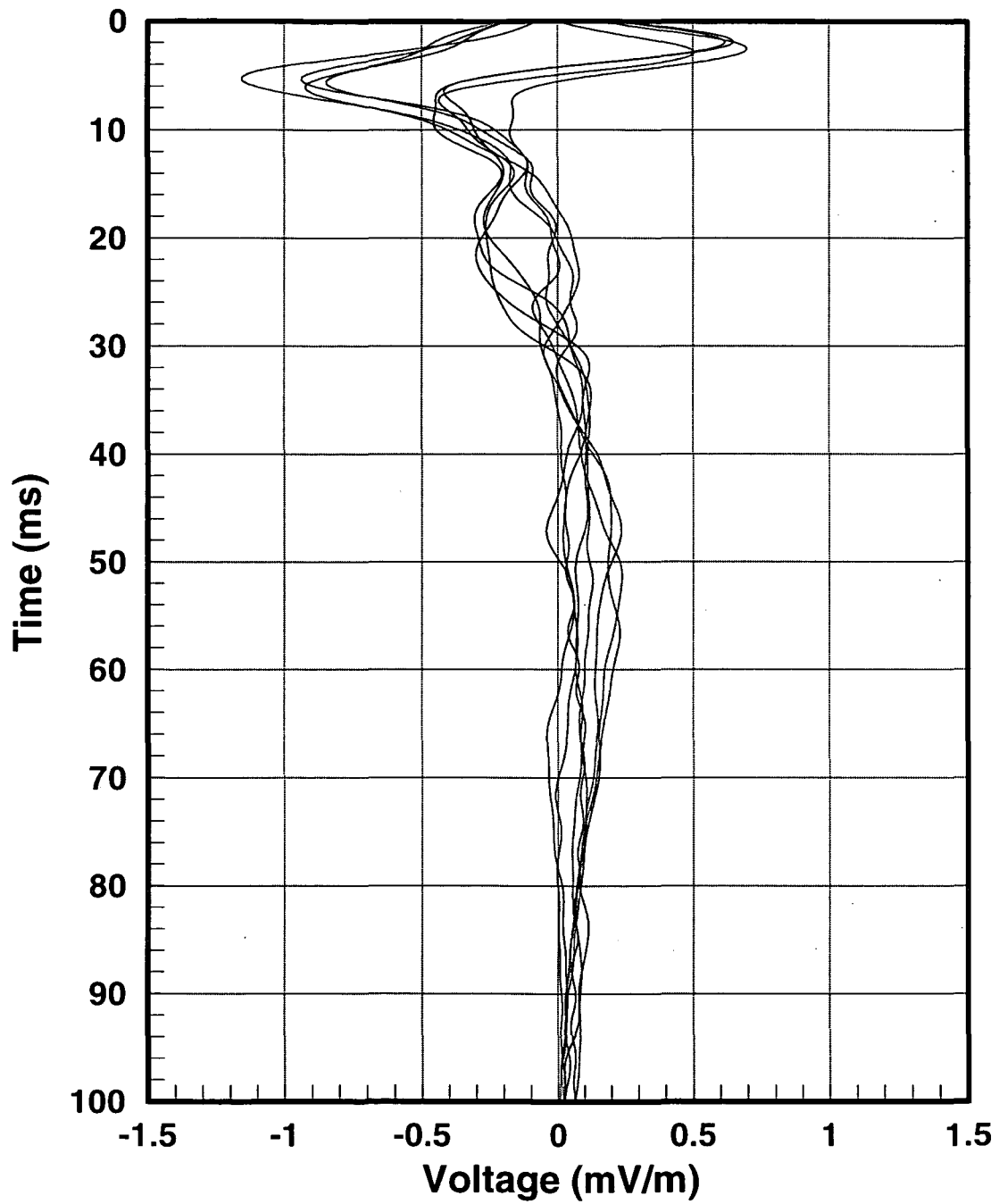
NIZ-B (Dyno) shots 21-24 (24 omitted in b)

Figure 3.2 EK sounding at Site B



NIZ-B (Dyno) shots 35-37 (2 channels)

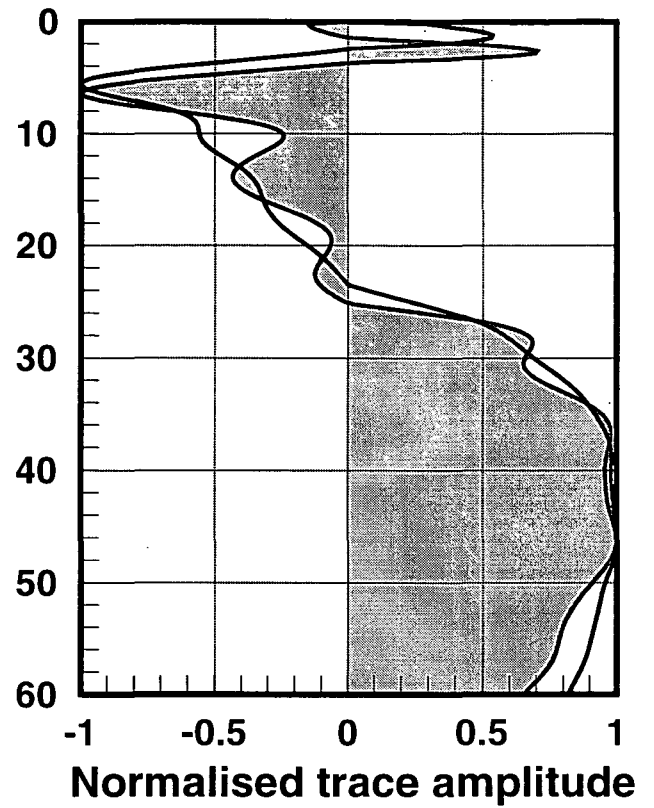
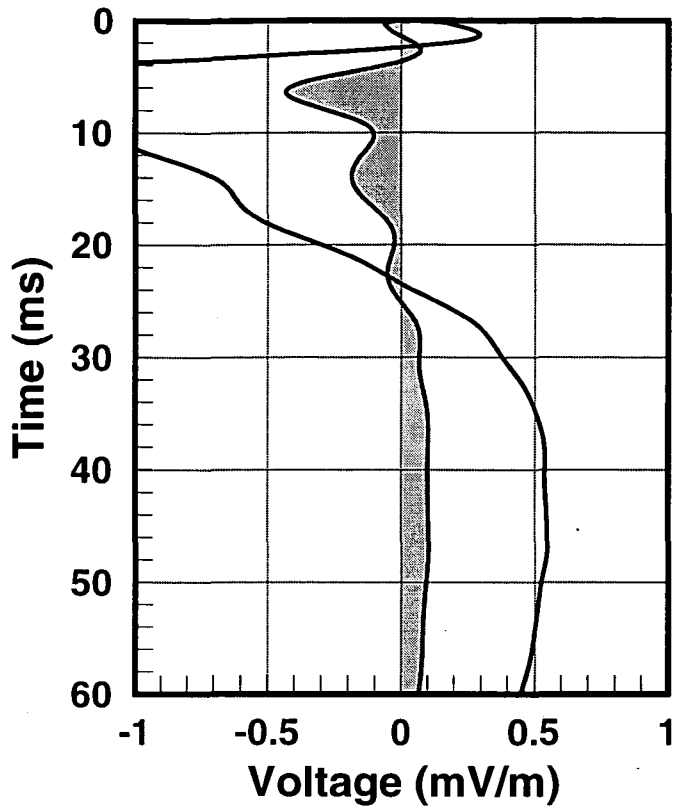
Figure 3.3 EK sounding at Site B



NIZ-B (Hammer) shots 4-7 (2 channels)

Figure 3.4 EK sounding at Site B

a) Hammer



b) Dynasource

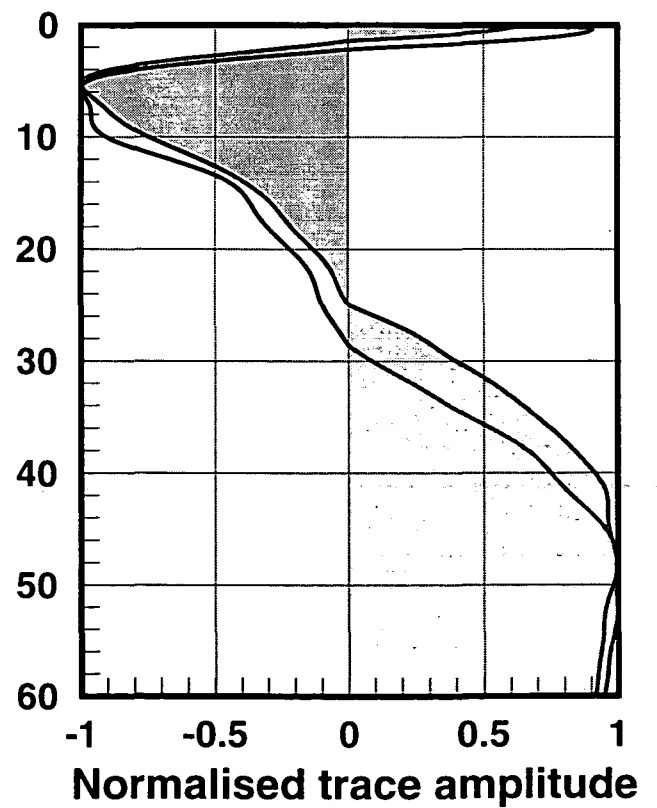
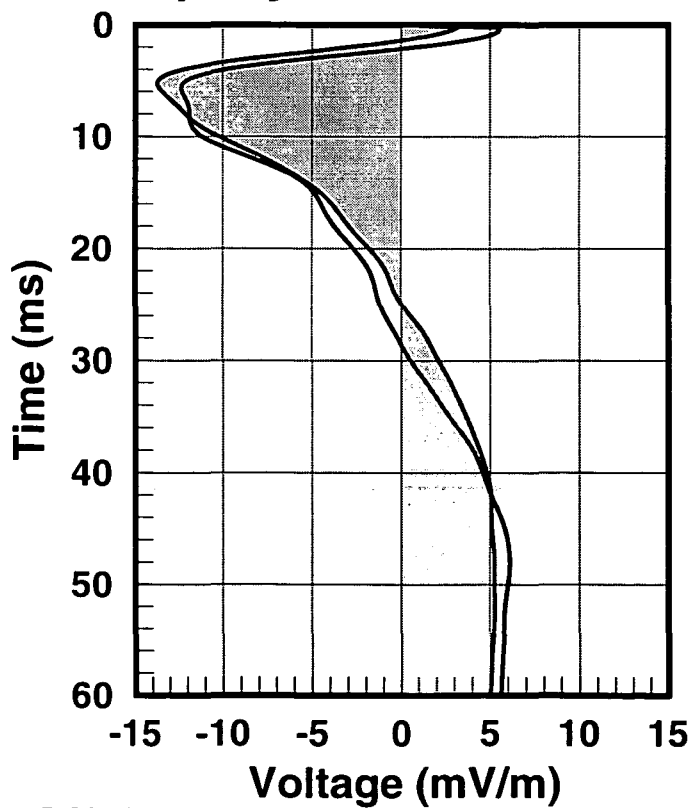
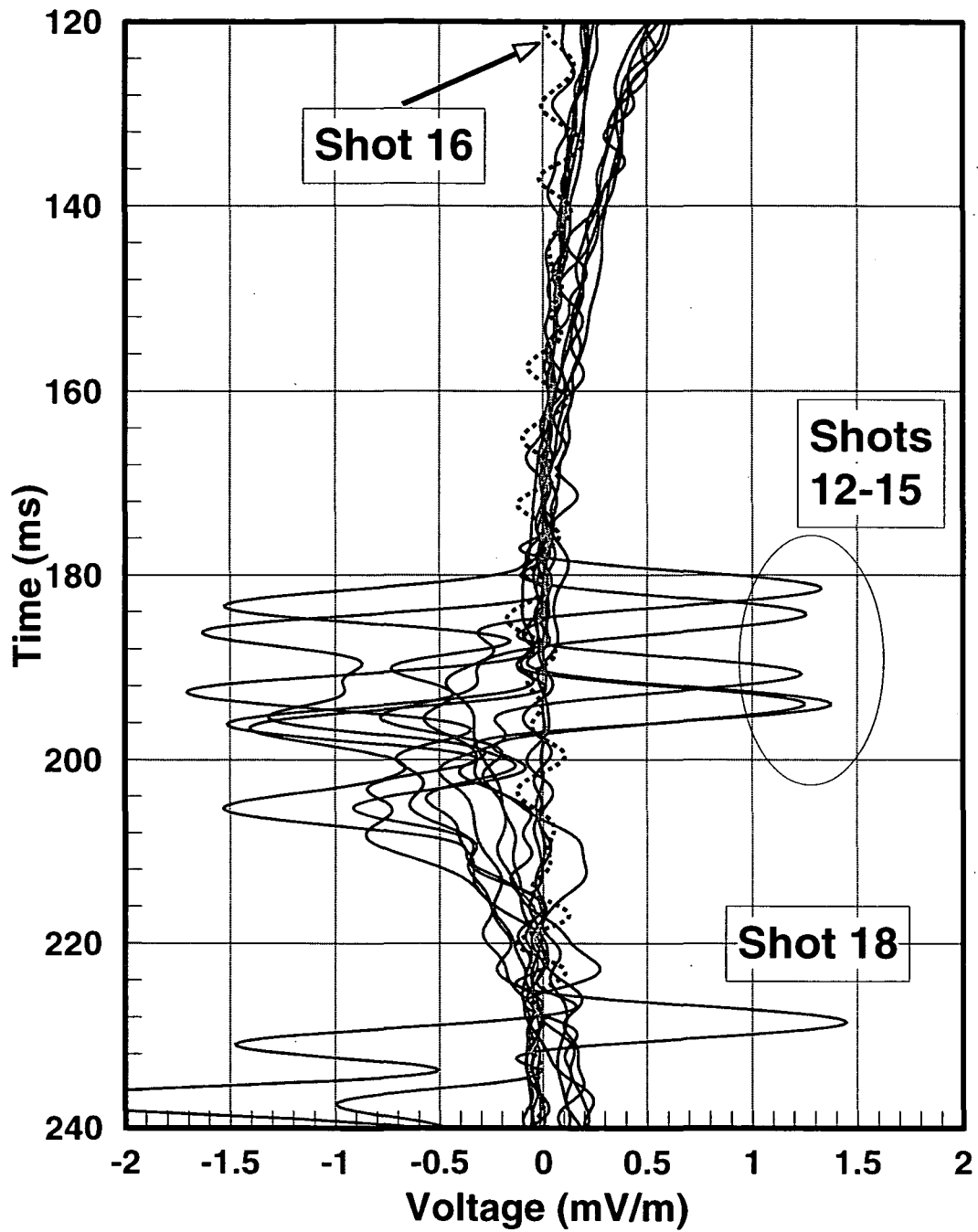
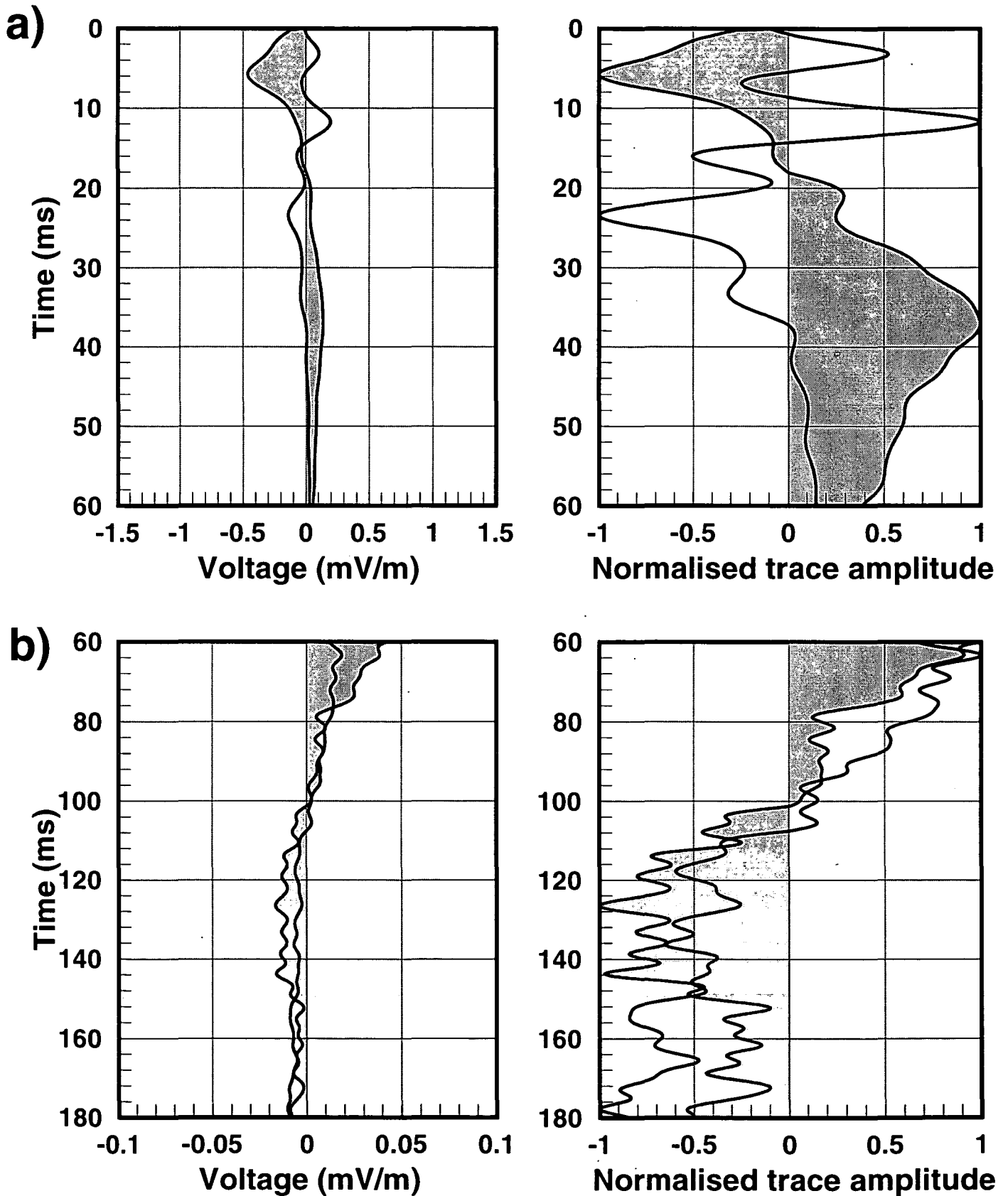


Figure 3.5 EK siunding at site E



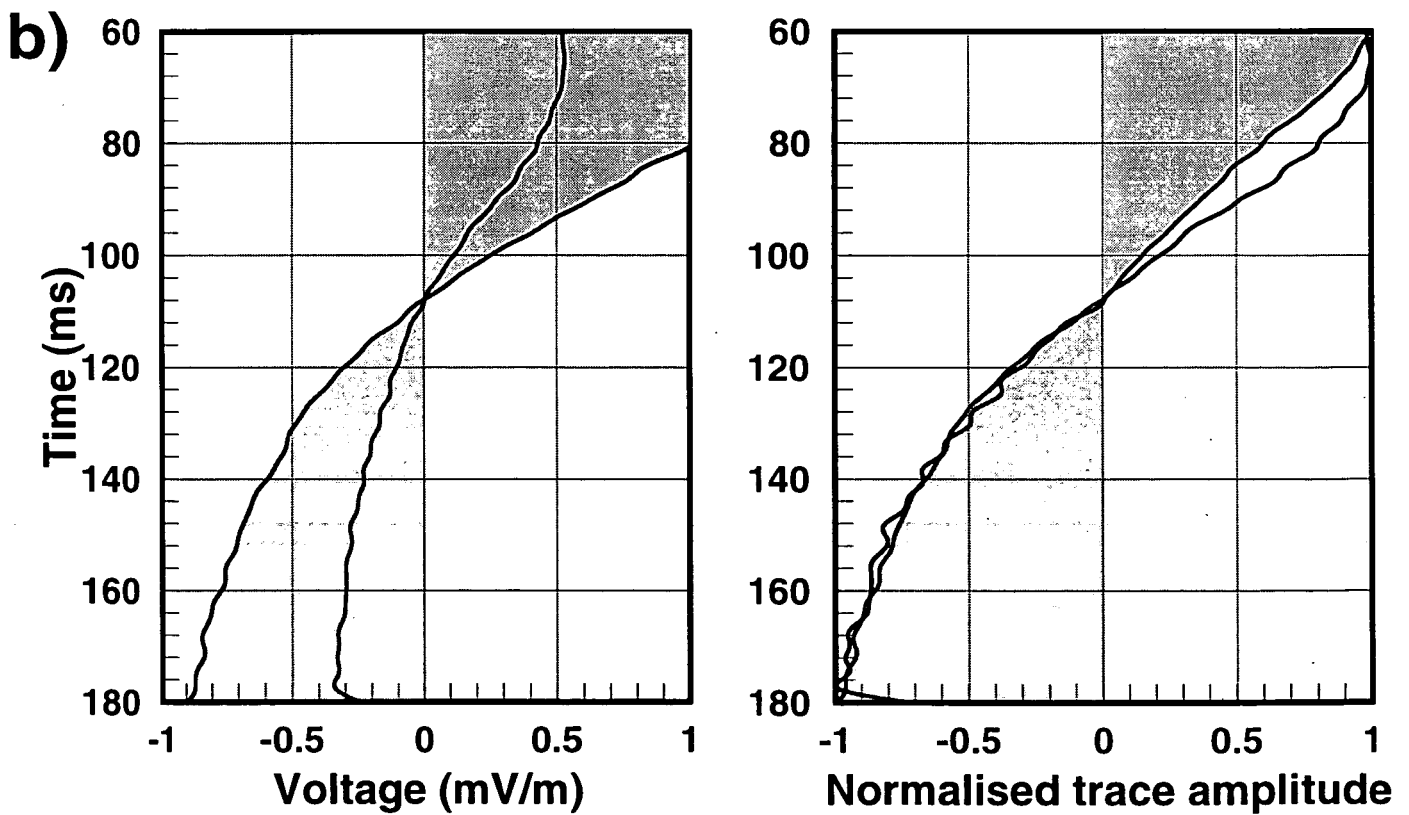
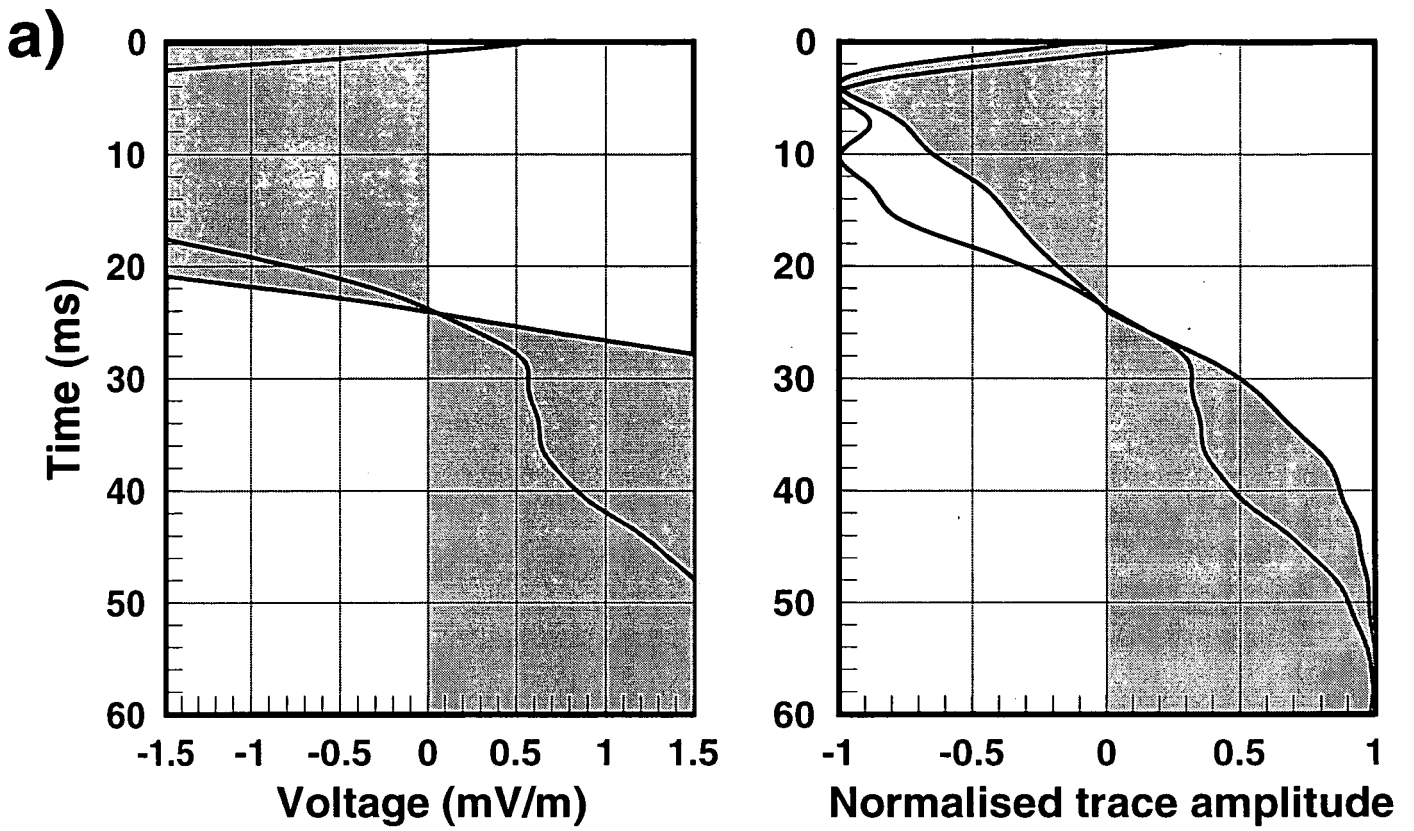
NIZ-E (Dyno) shots 12-18. 2-channels

Figure 3.6 EK sounding at site E



NIZ-E (hammer)

Figure 3.7 EK sounding at site E



NIZ-E (dyno)

Fig. 4.1

Figure 4.1 Site D. First three channels
1&2=blue, 3&4=red,5&6=black

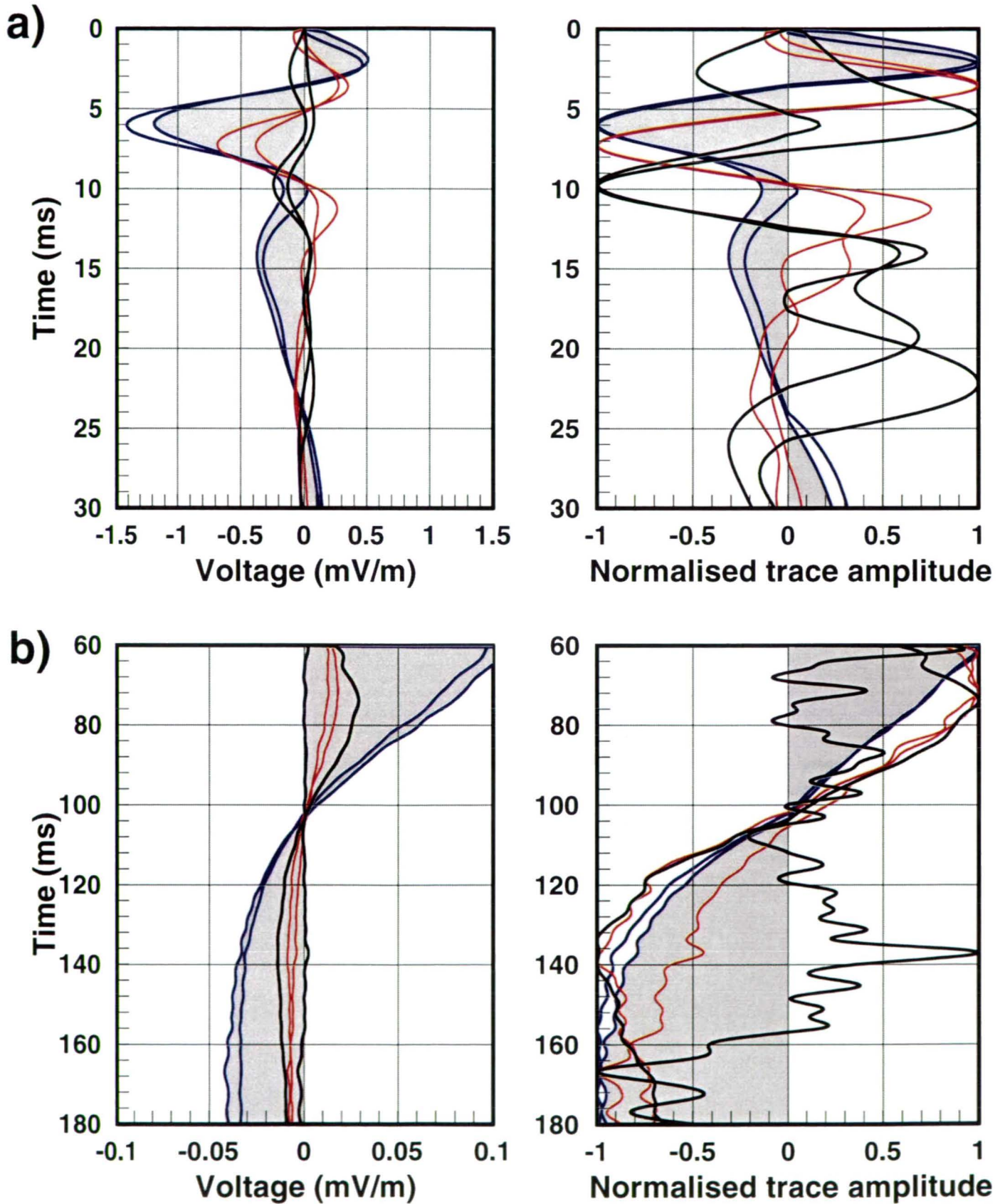
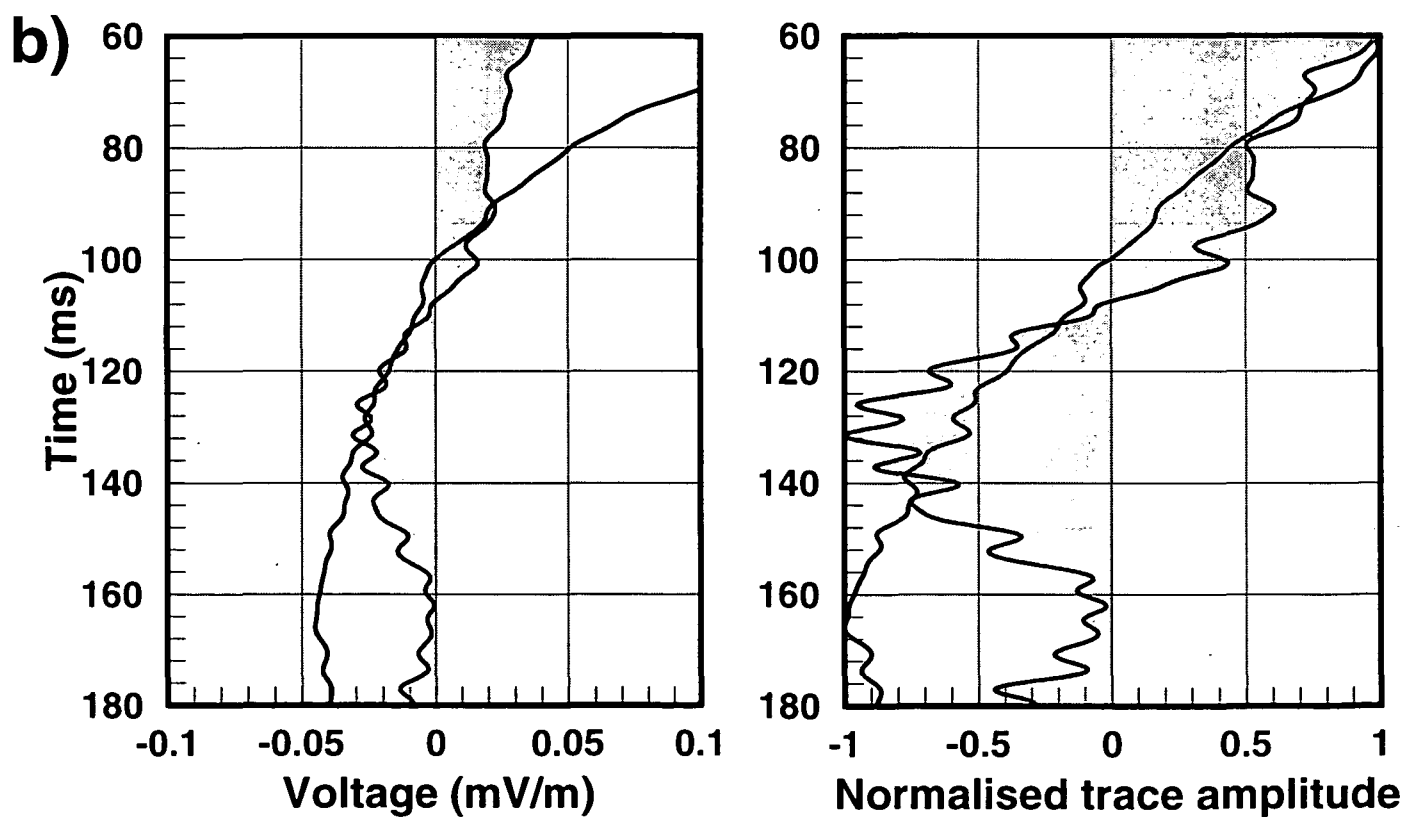
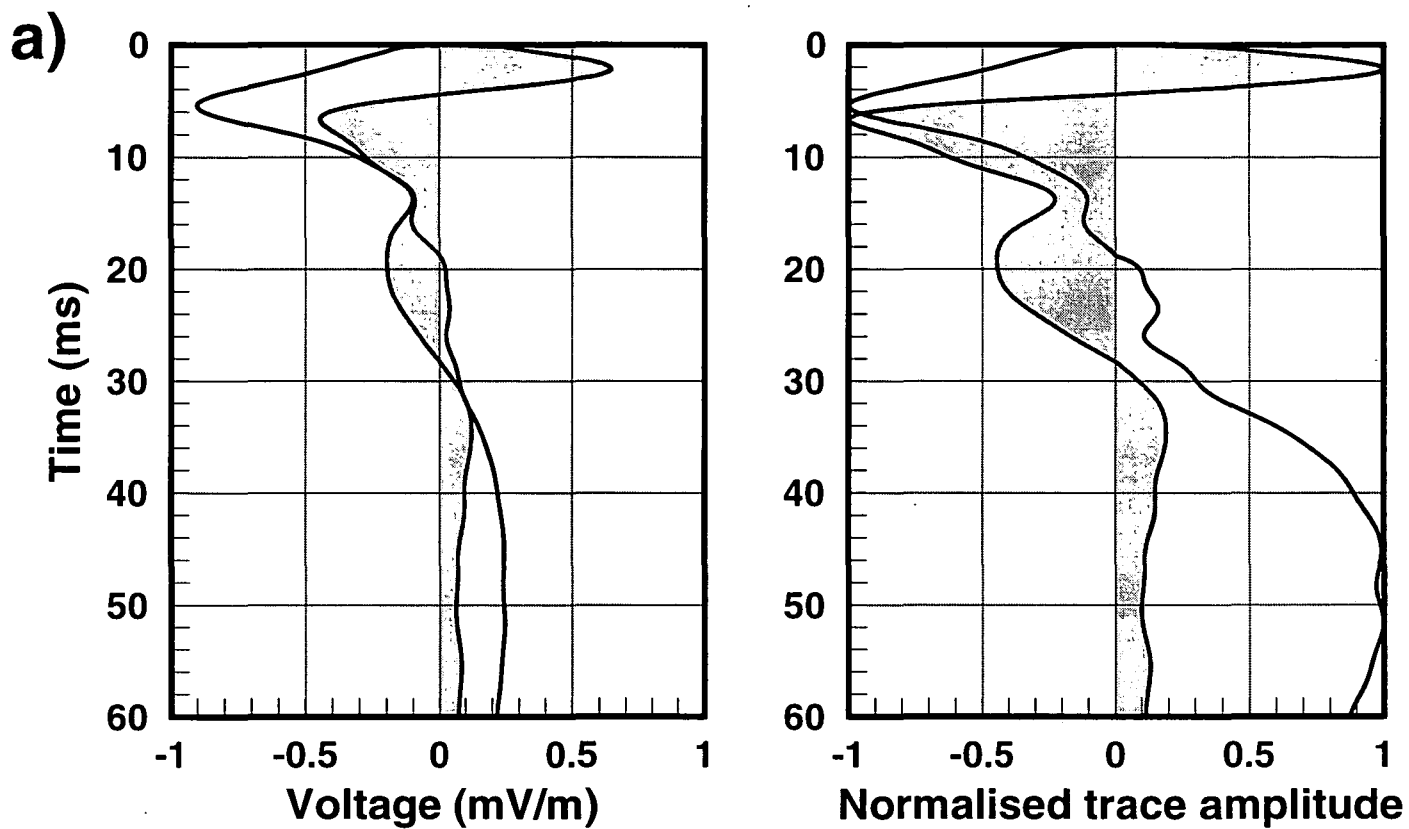
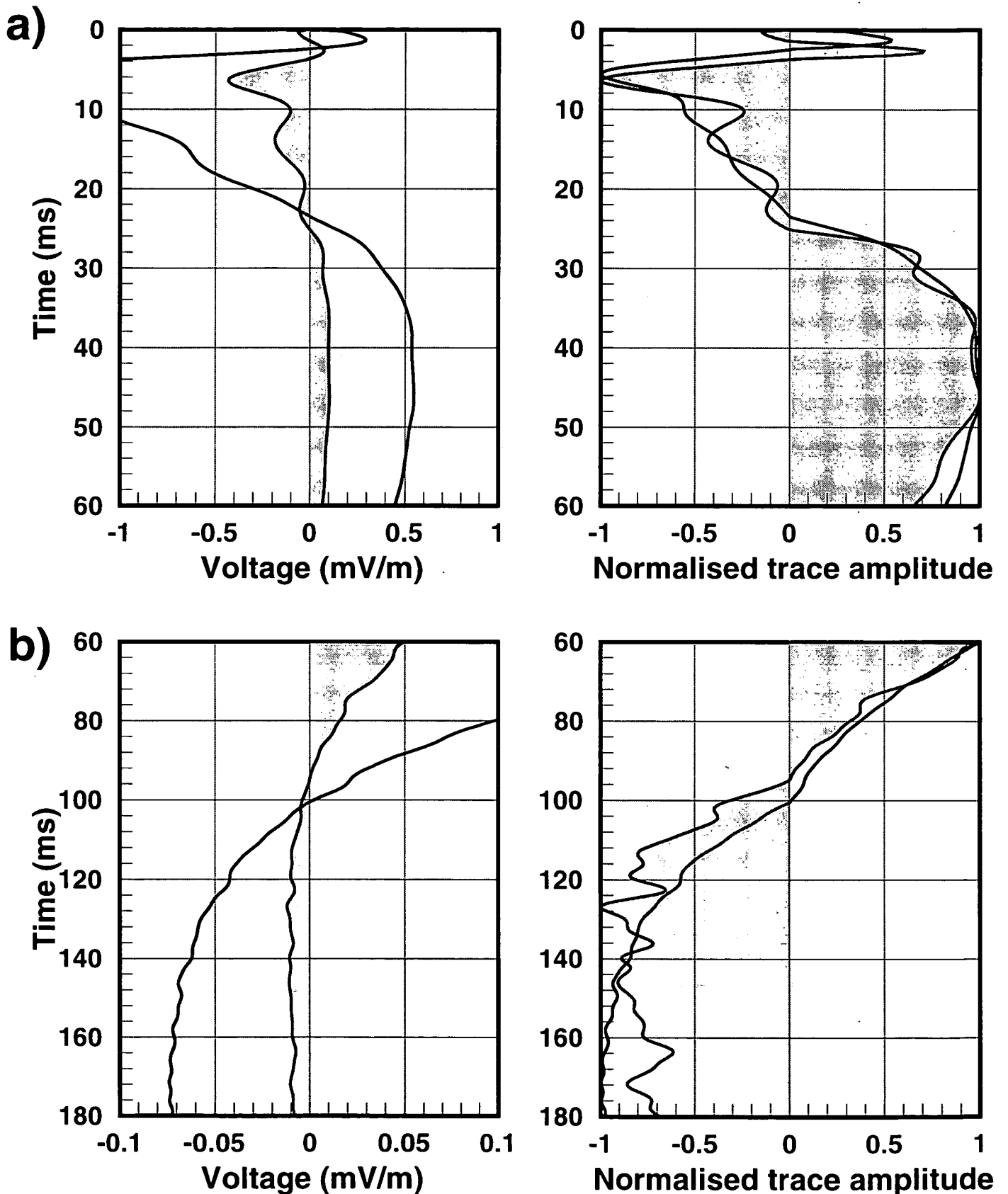


Figure 5.1 EK sounding at site A



NIZ-A

Figure 5.2 EK sounding at site B



NIZ-B

Figure 5.3 EK sounding at site C

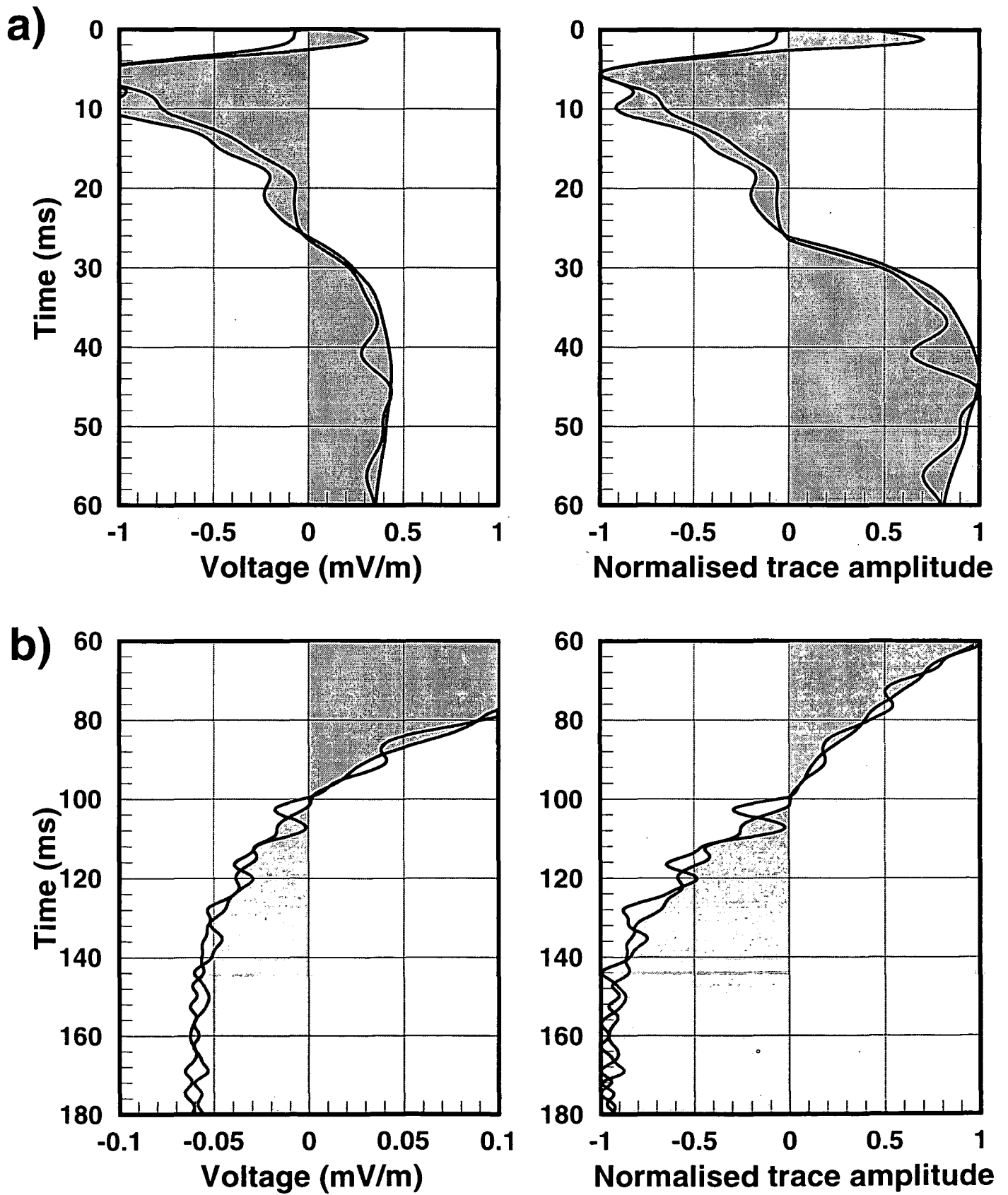


Figure 5.4 EK sounding at site D

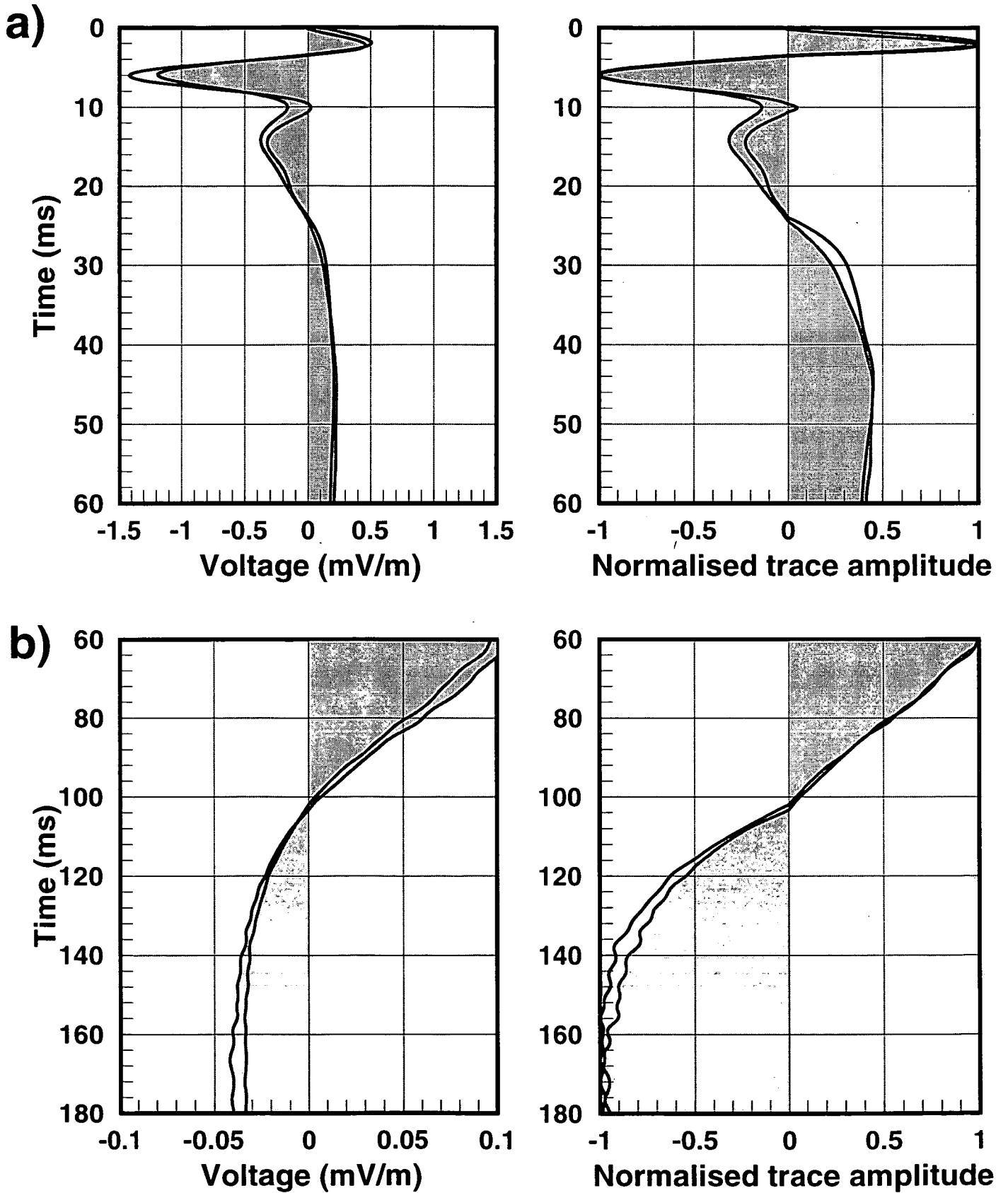
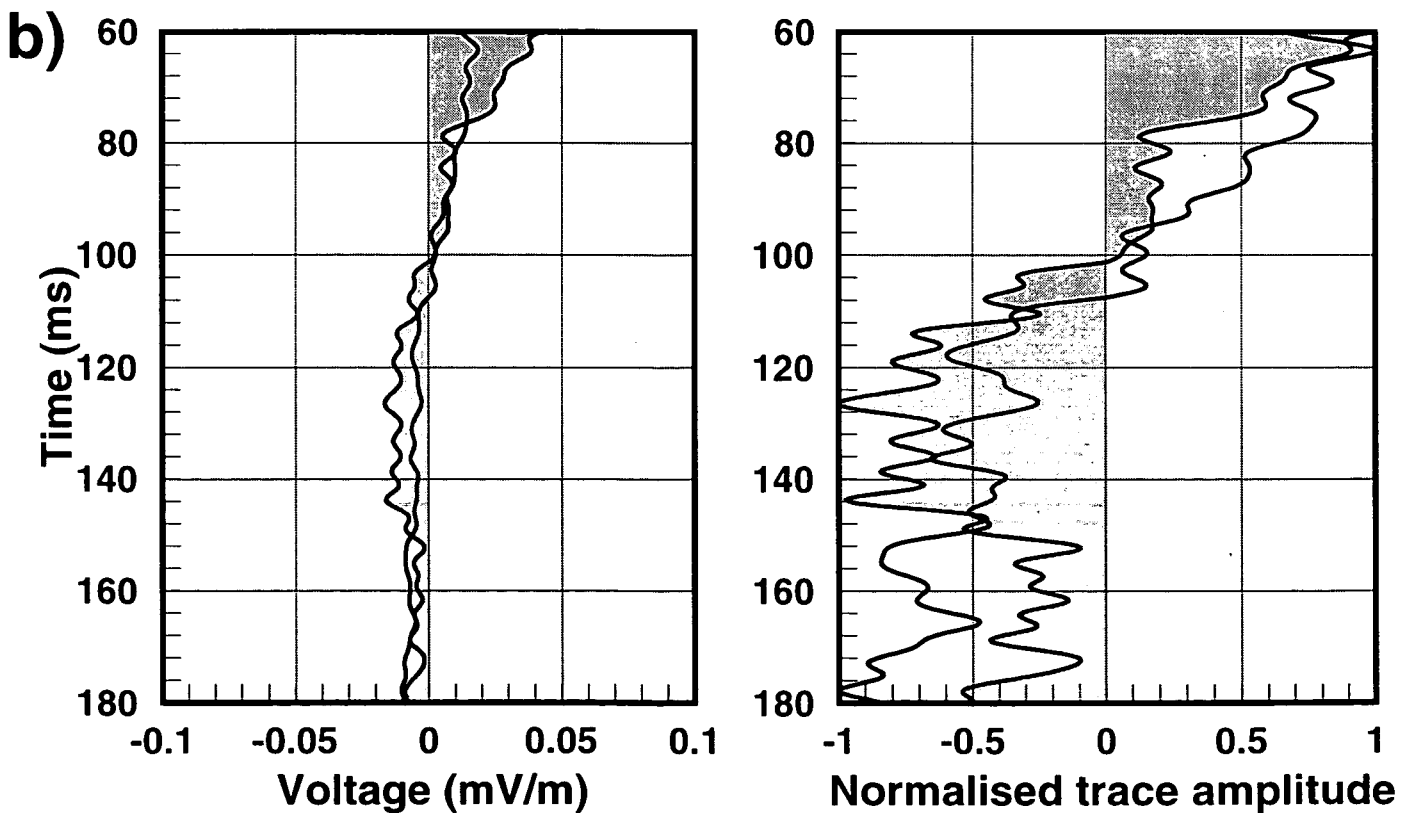
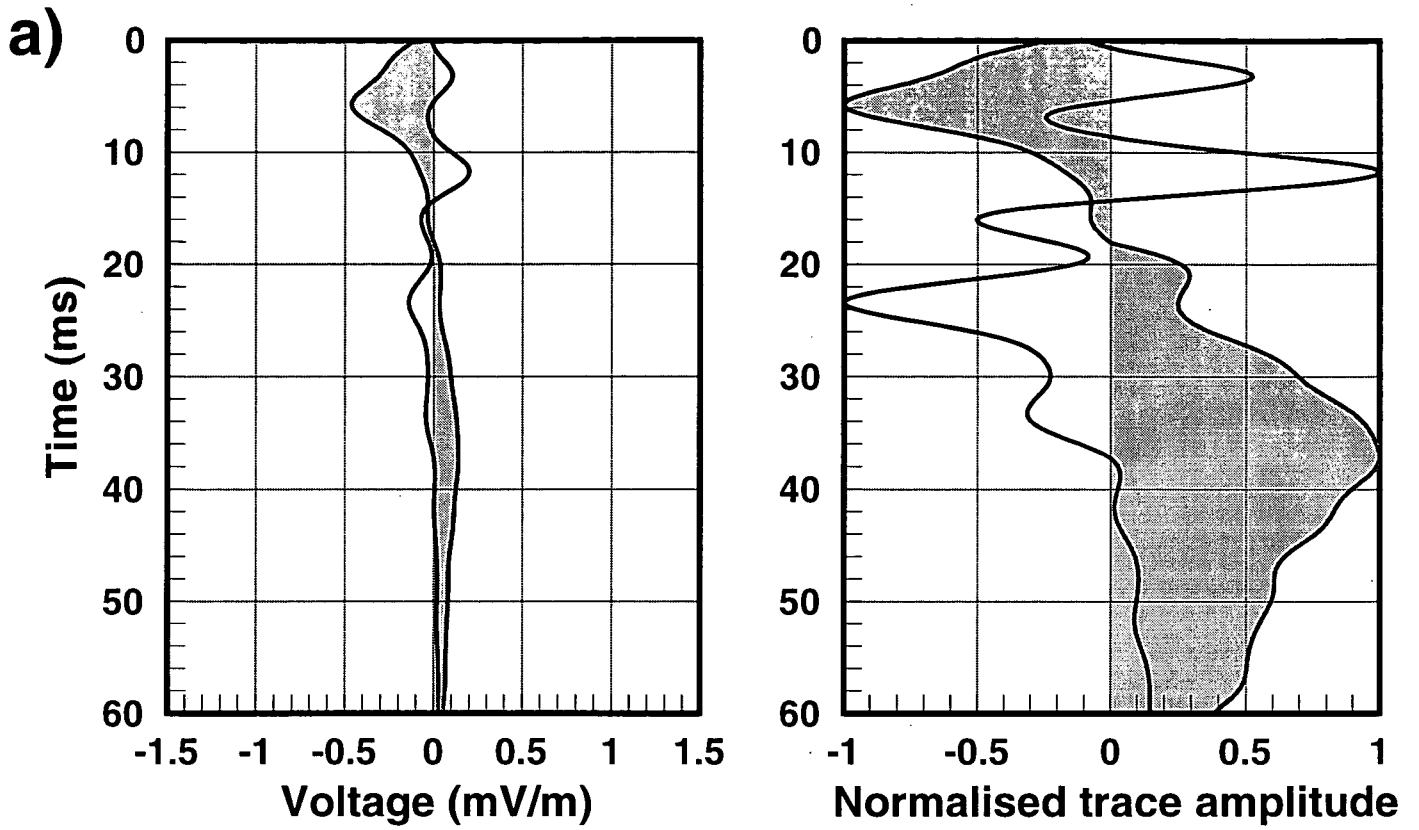
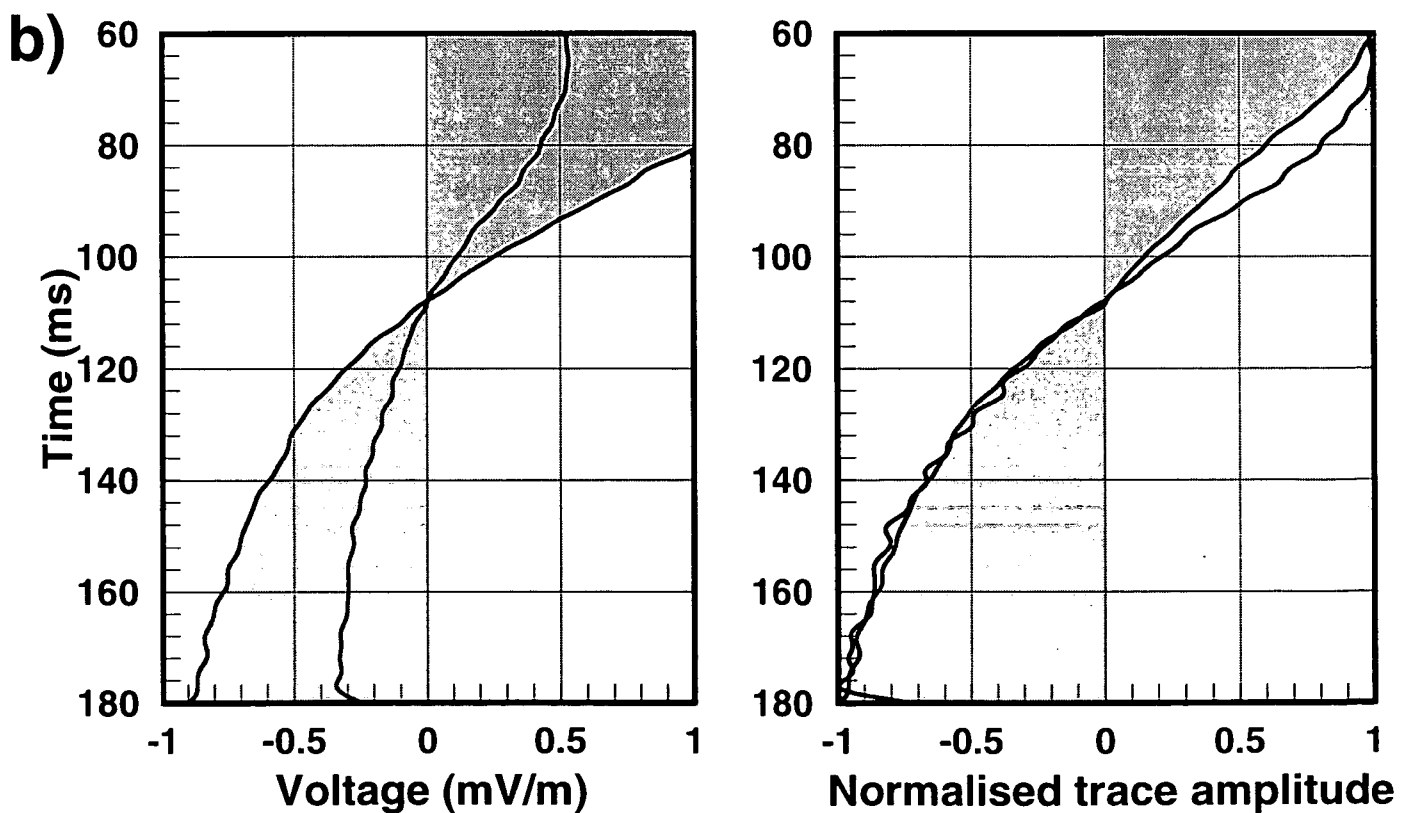
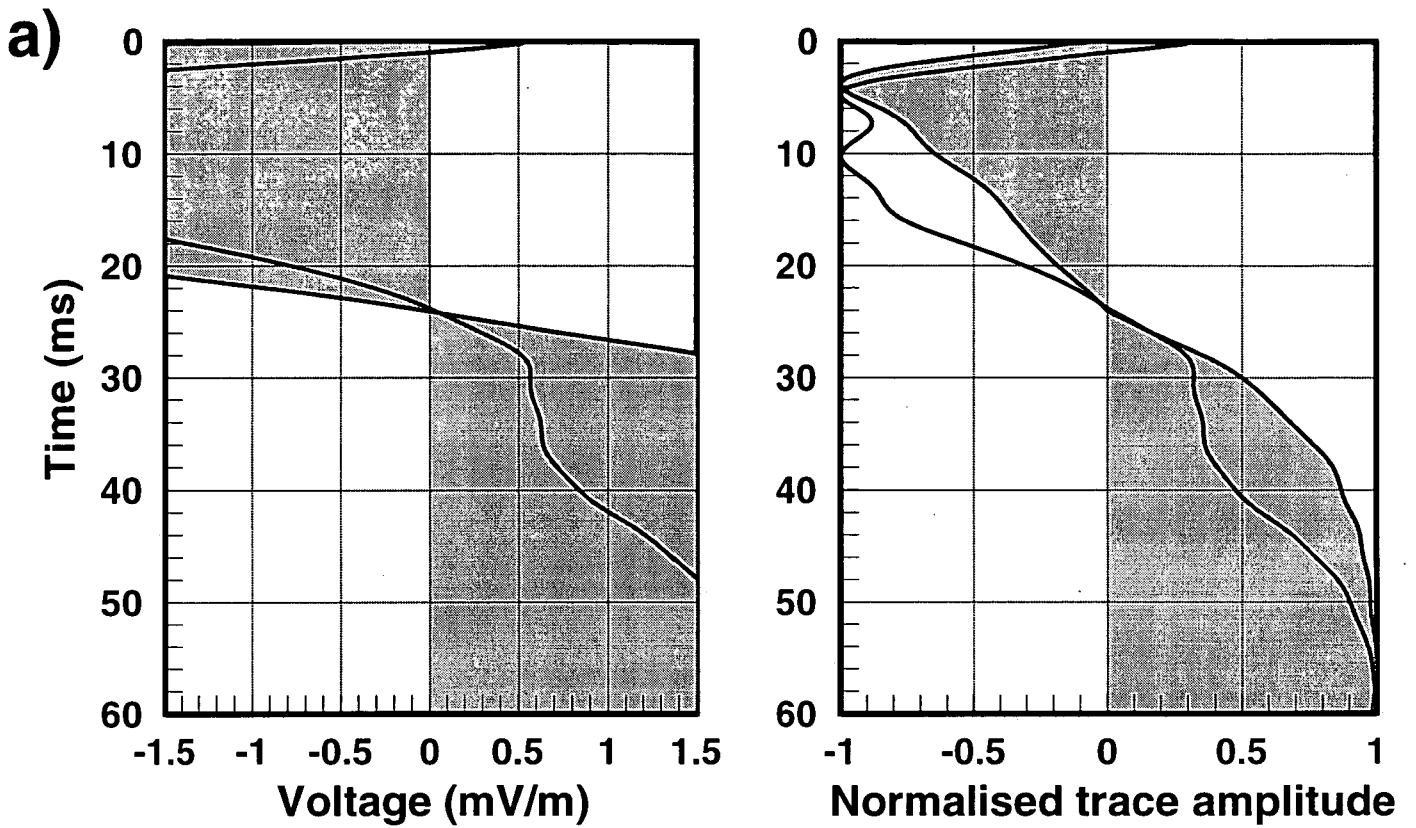


Figure 5.5 EK sounding at site E (hammer)



NIZ-E (hammer)

Figure 5.6 EK sounding at site E (dyno)



NIZ-E (dyno)

Figure 5.7 EK sounding at site F

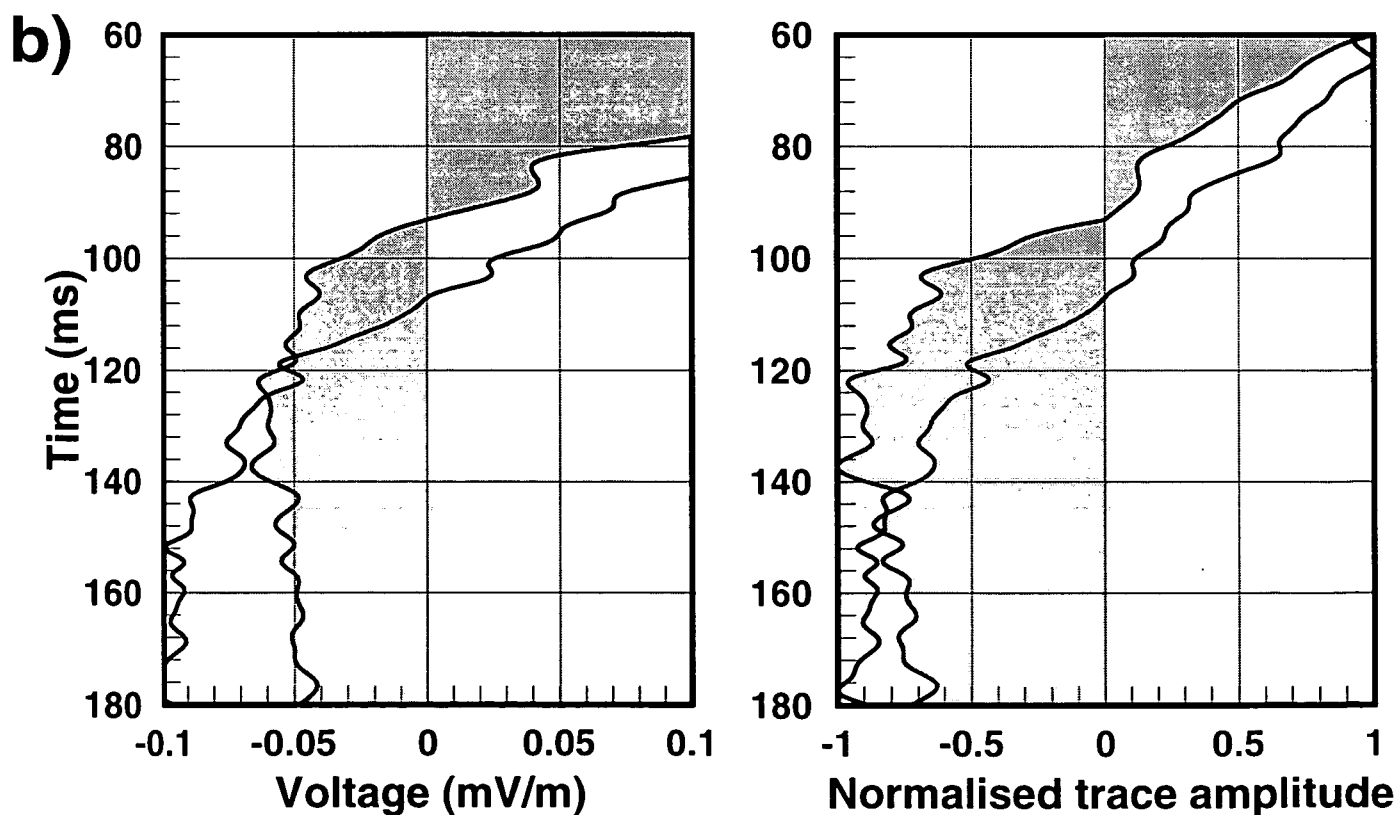
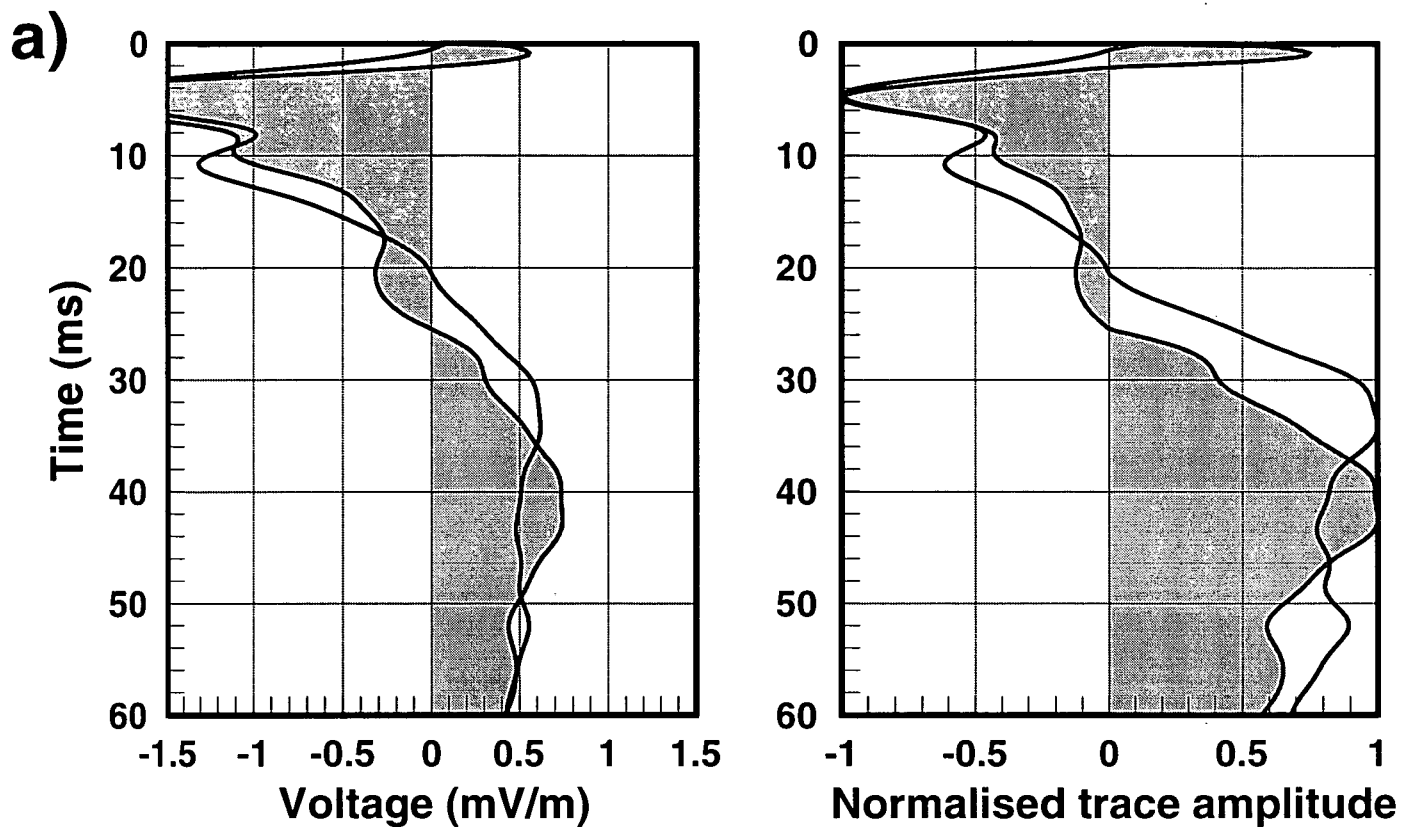


Figure 5.8 EK sounding at site G

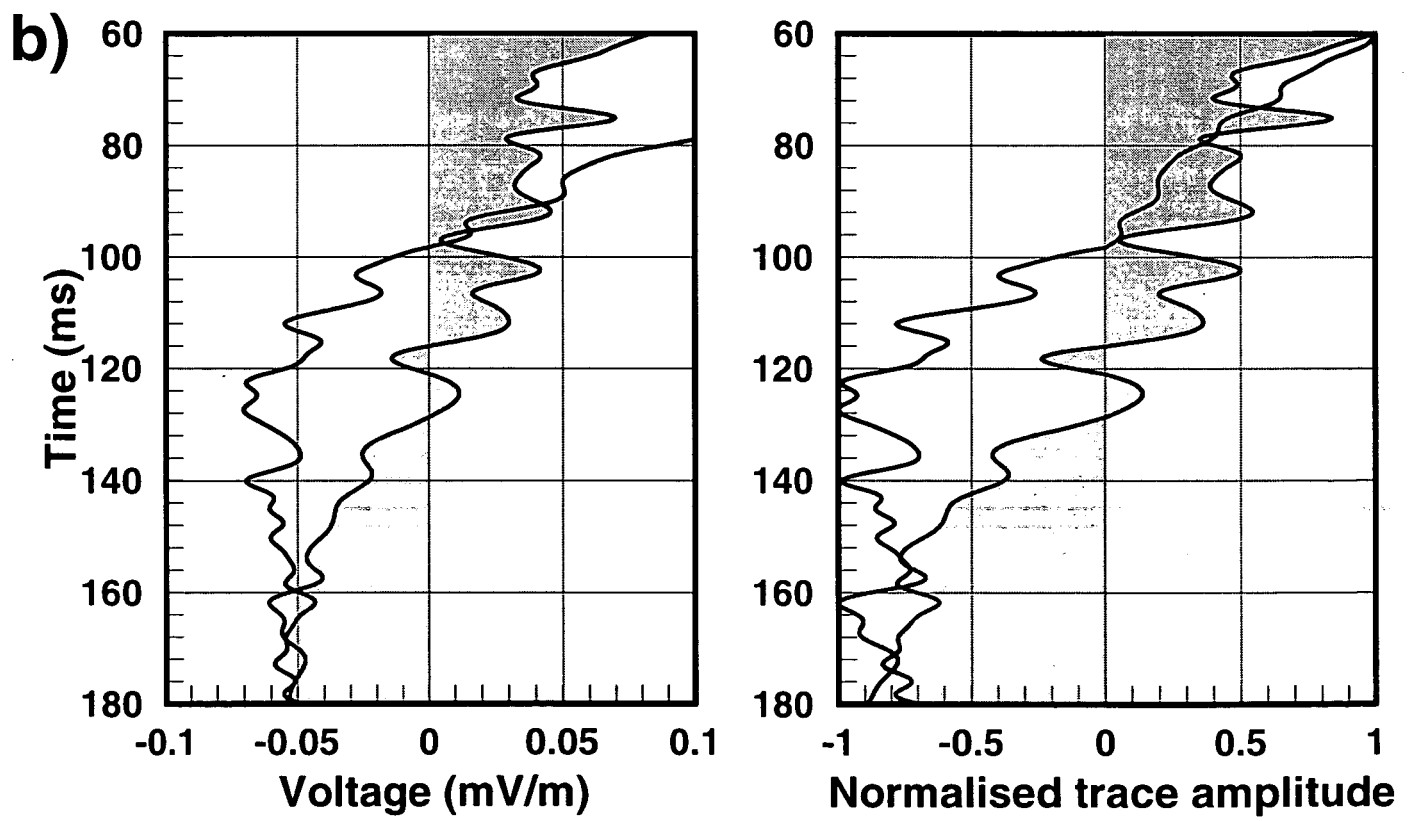
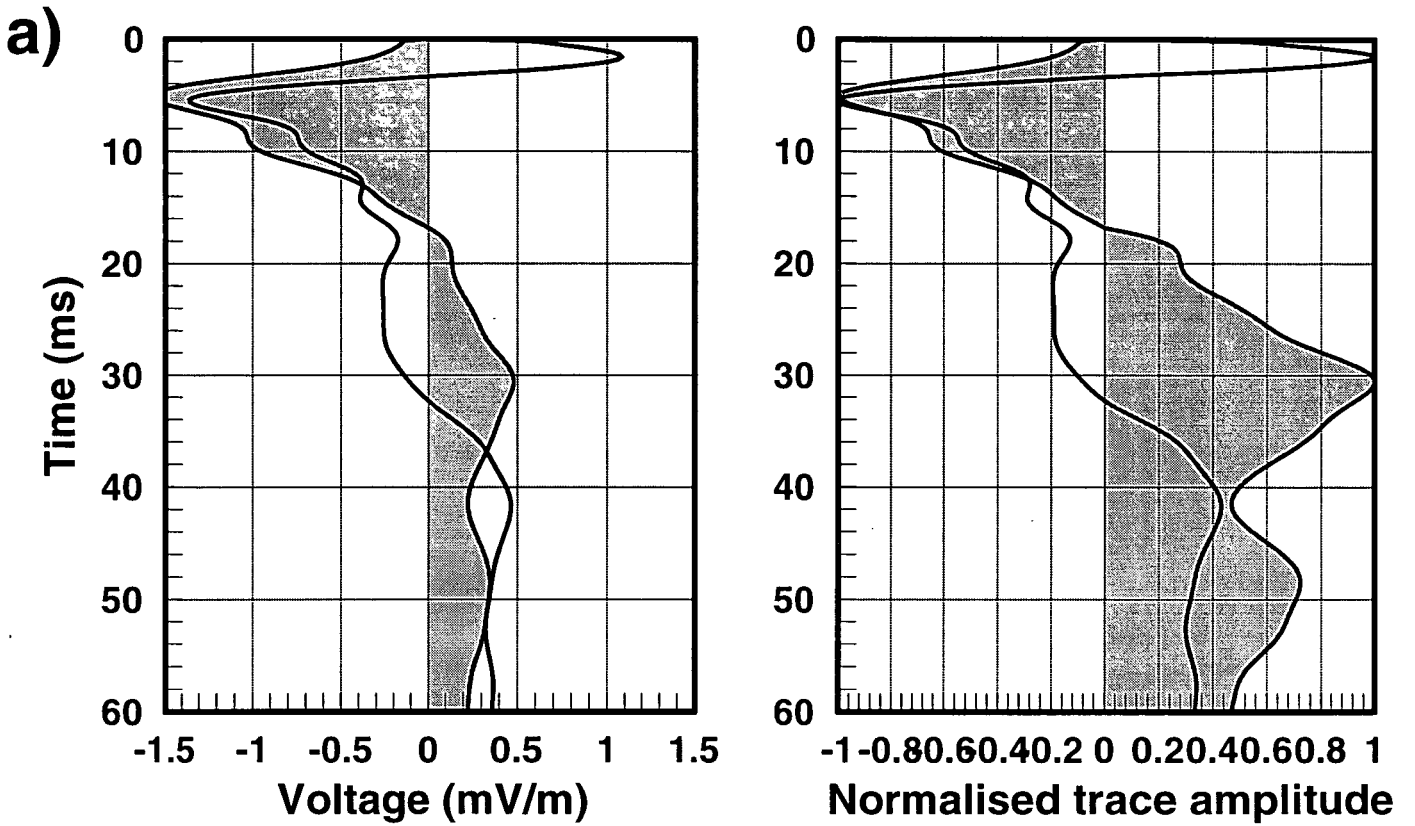
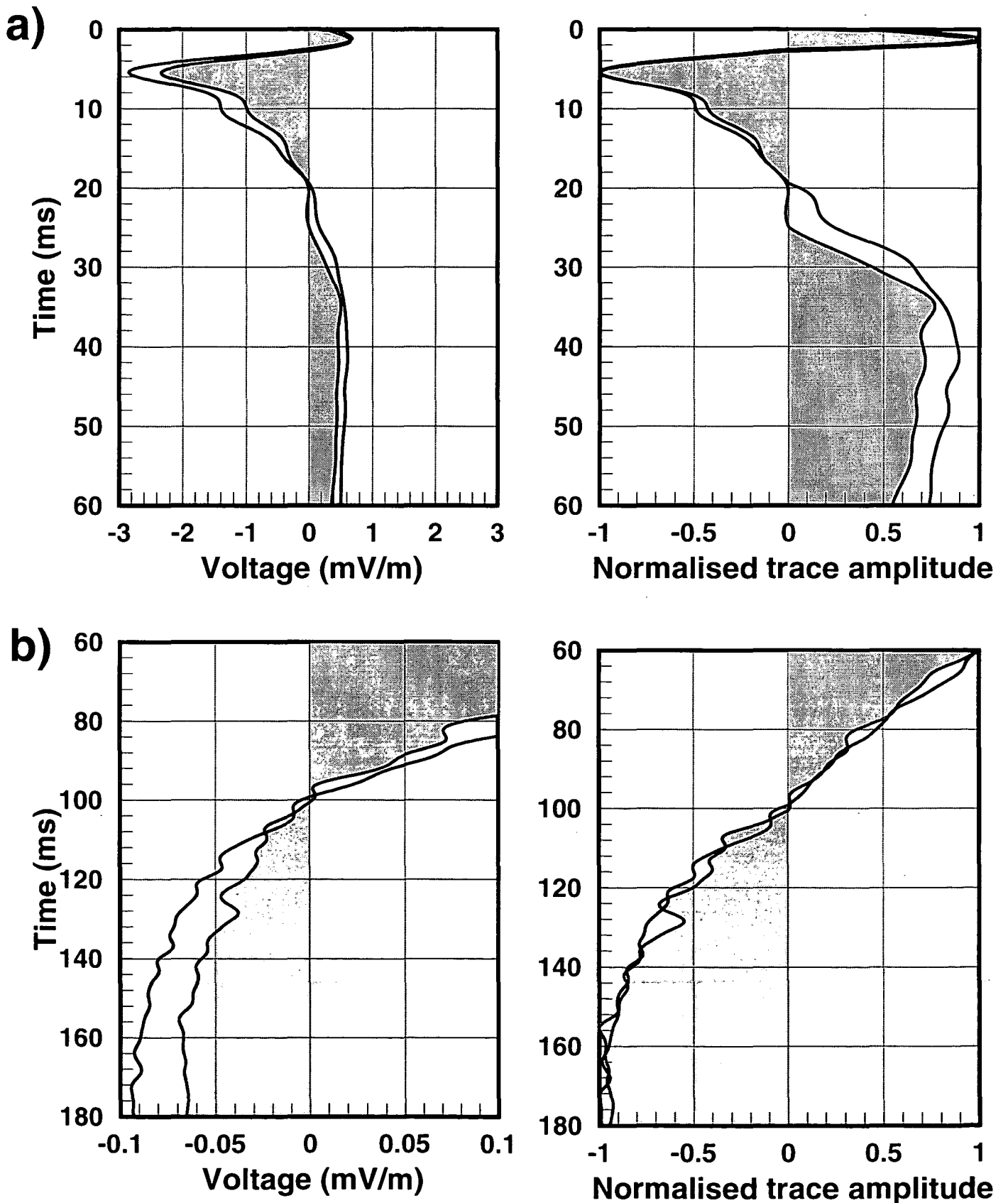


Figure 5.9 EK sounding at site H



NIZ-H

Figure 5.10 EK sounding at site I

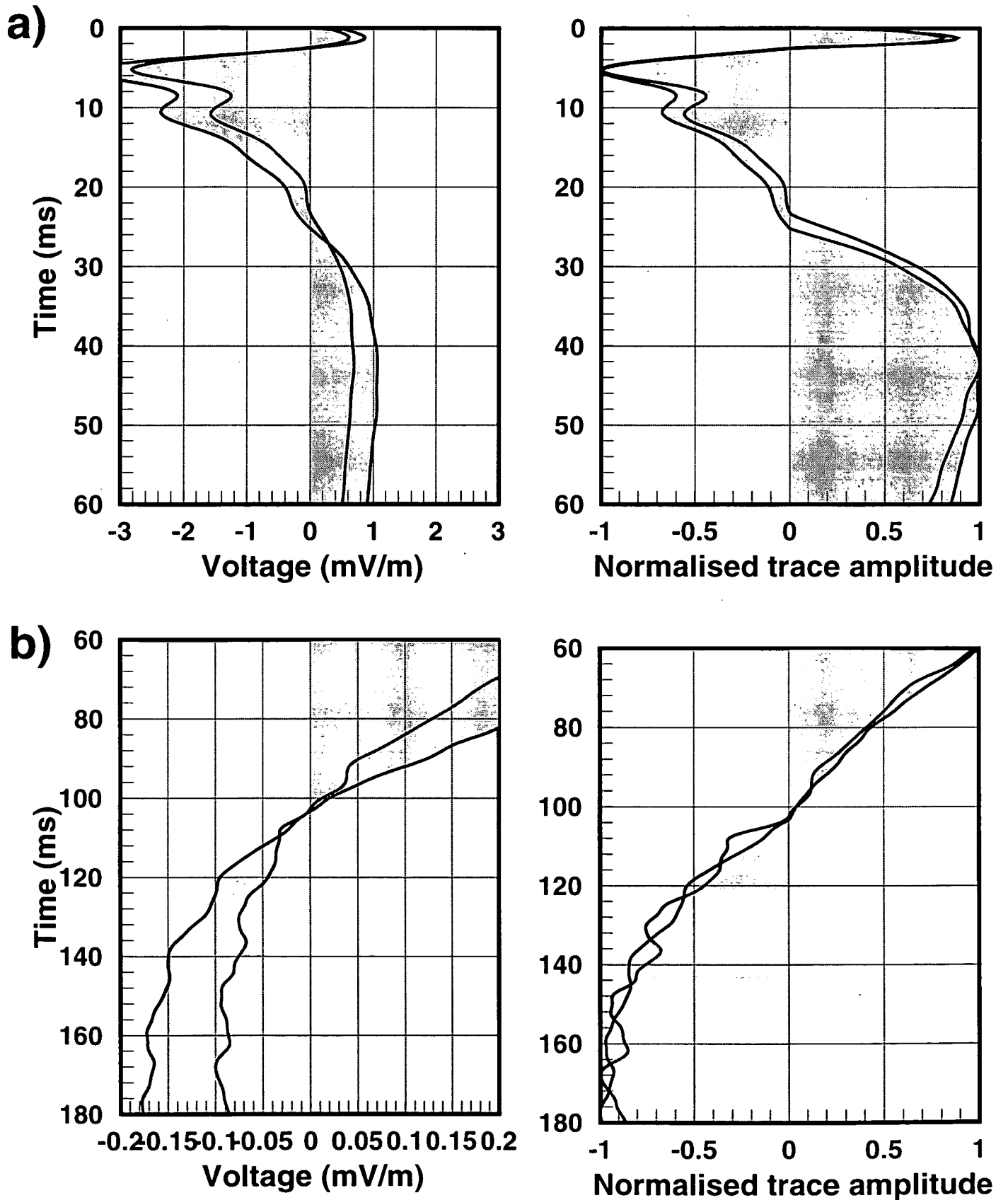


Figure 6.1. EK estimated, normalised hydraulic conductivity at sites a) NIZ-A and b) NIZ-B

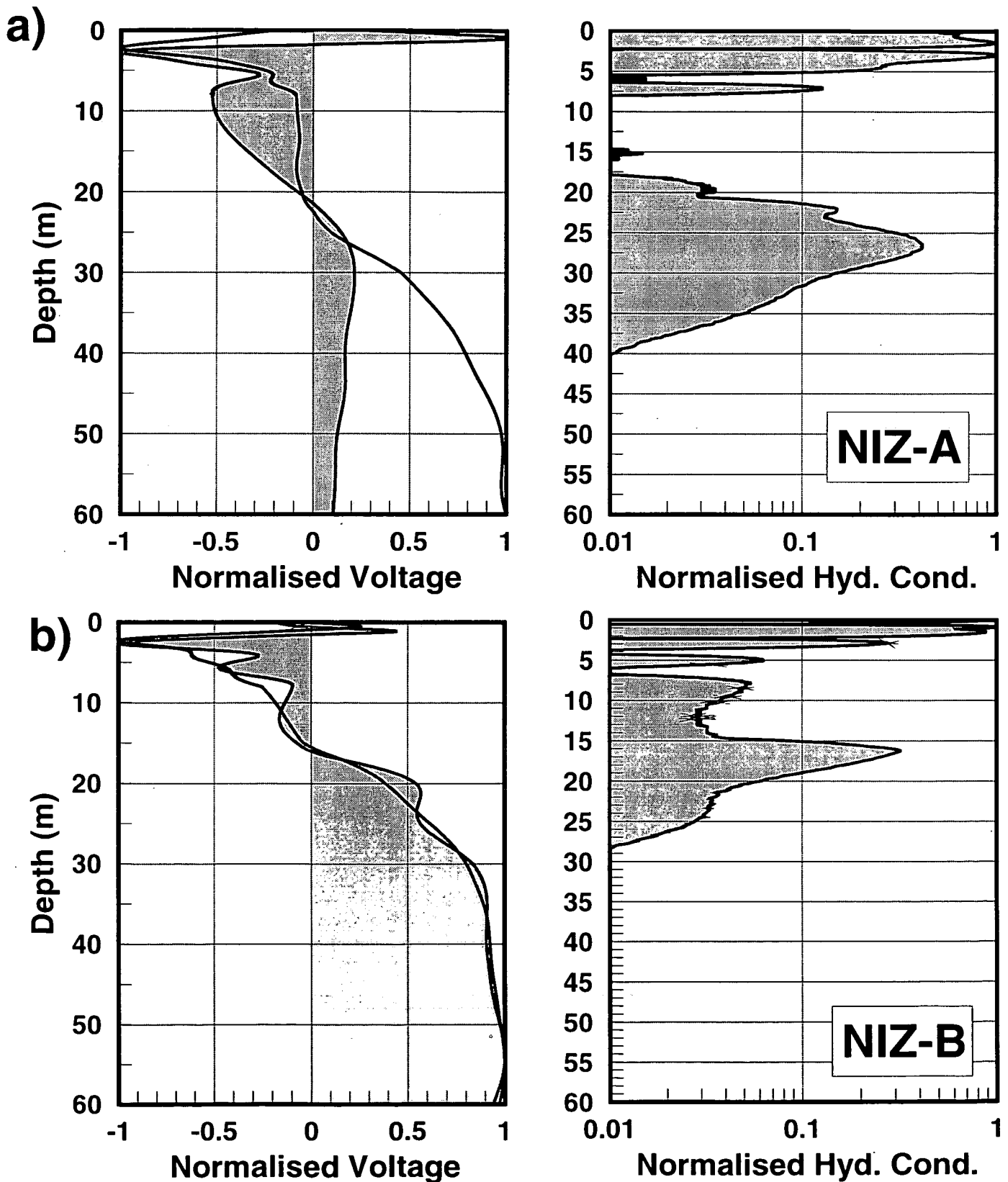


Figure 6.2. EK estimated, normalised hydraulic conductivity at sites a) NIZ-C and b) NIZ-D

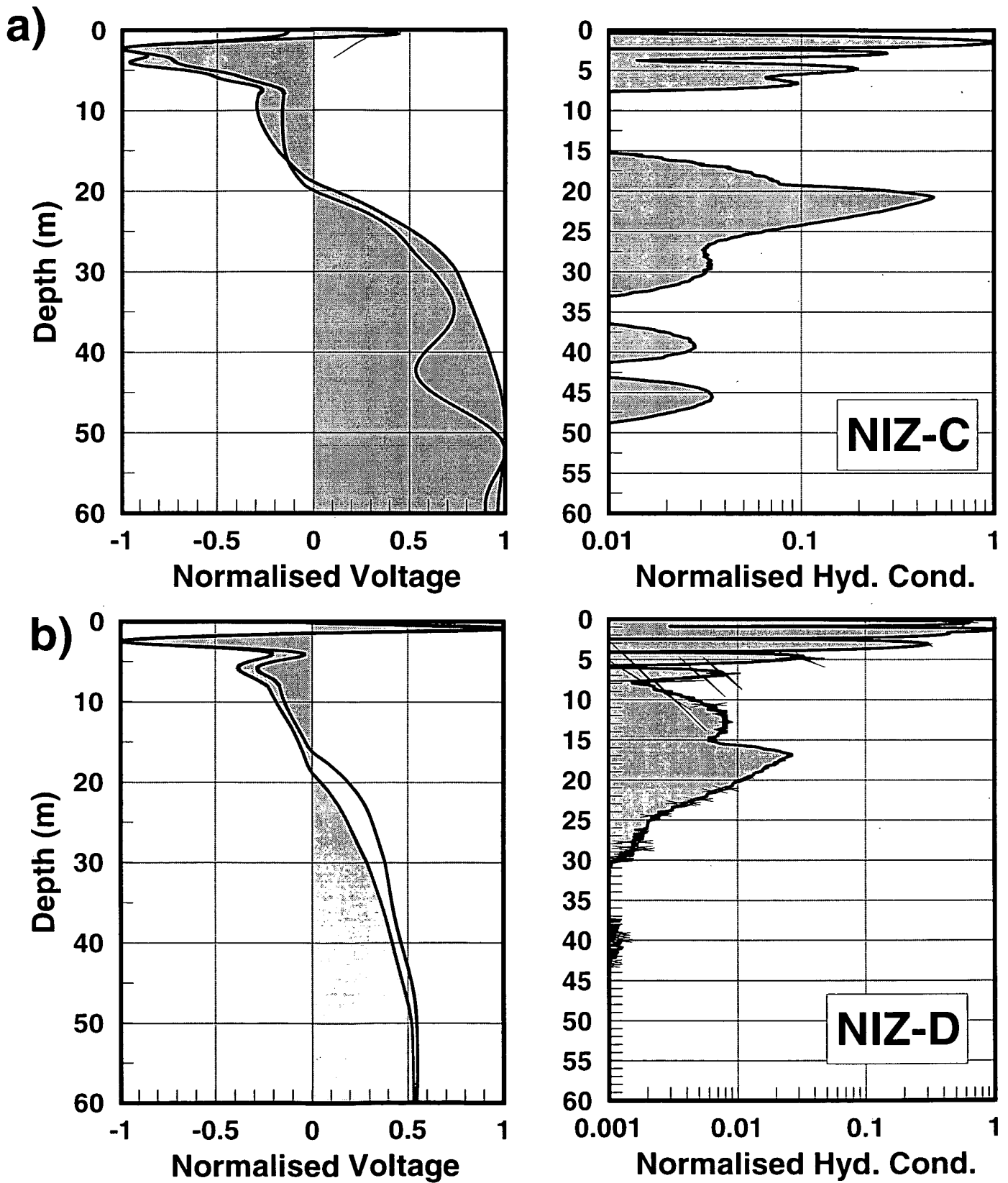


Figure 6.3. EK estimated, normalised hydraulic conductivity at sites a) NIZ-E and b) NIZ-F

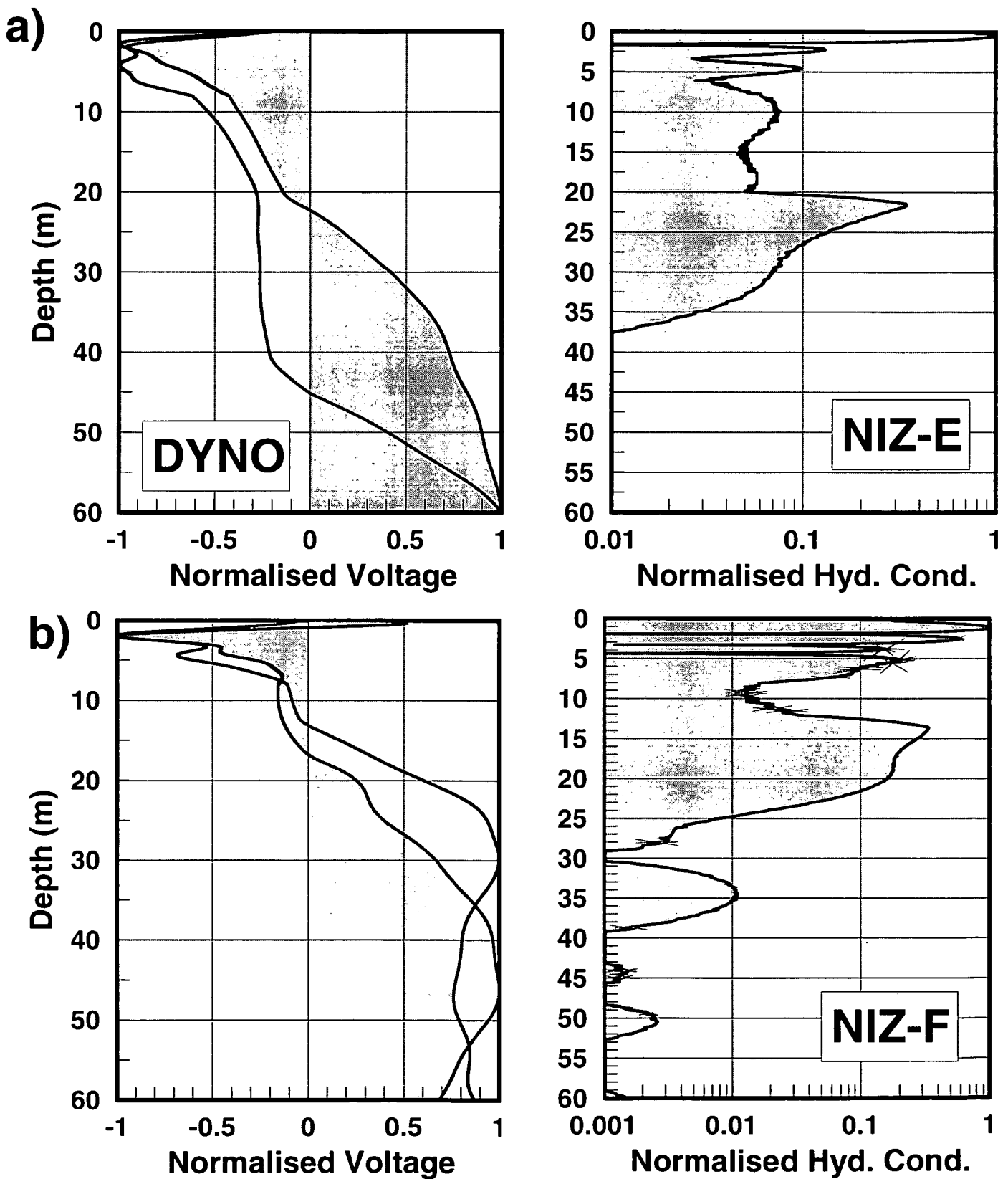


Figure 6.4. EK estimated, normalised hydraulic conductivity at sites a) NIZ-H and b) NIZ-I

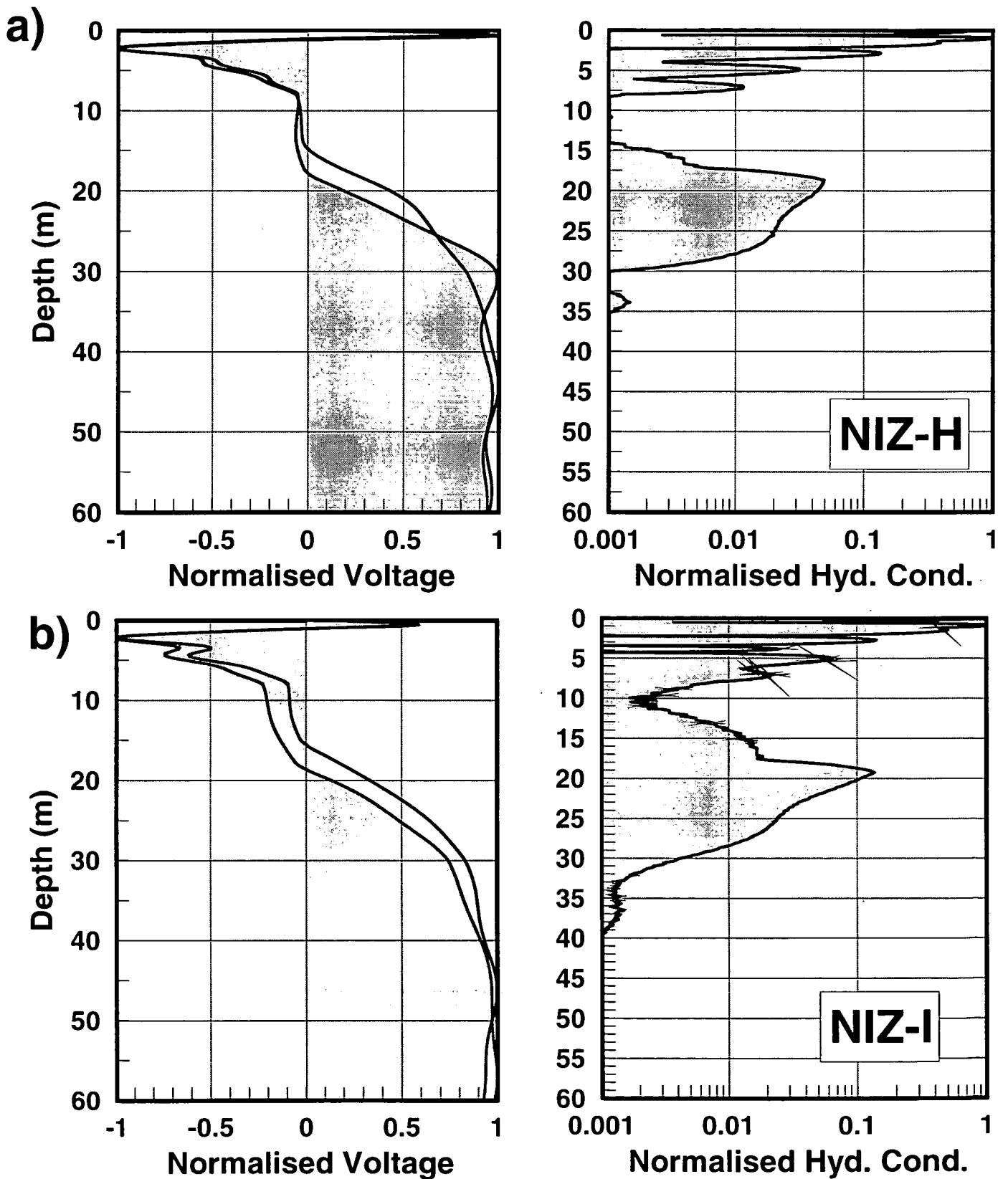


Figure 6.5. EK estimated, normalised hydraulic conductivity at 4 sites

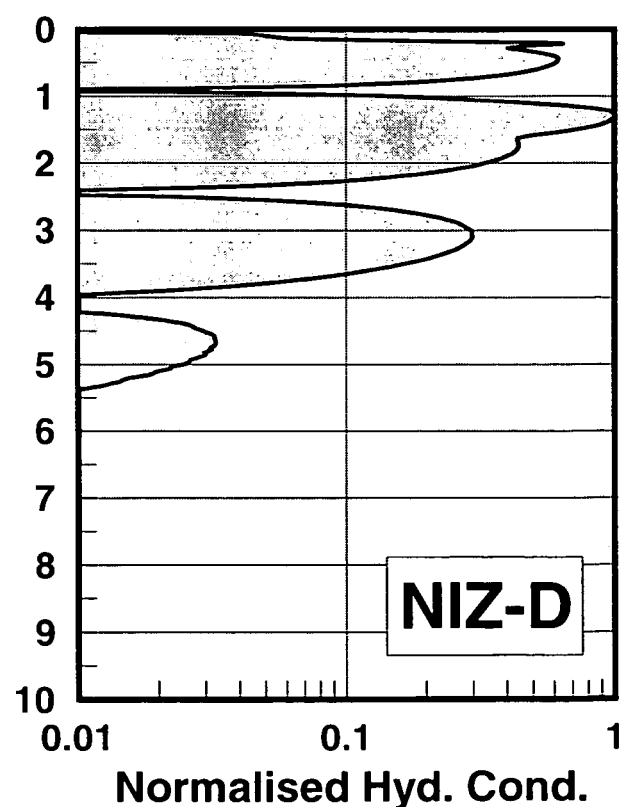
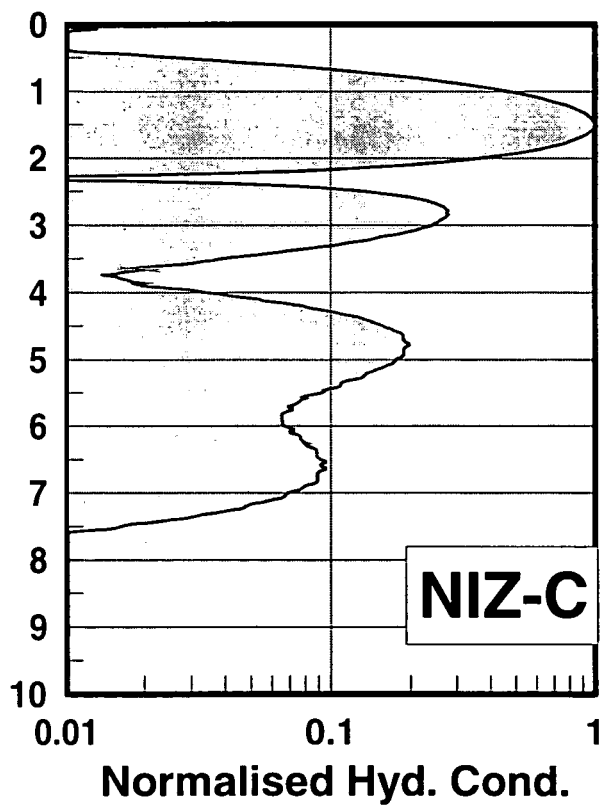
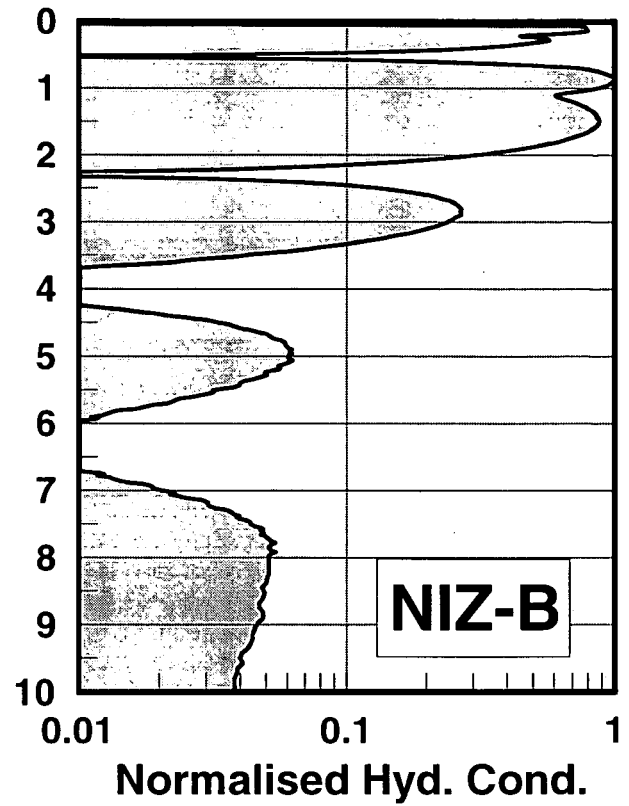
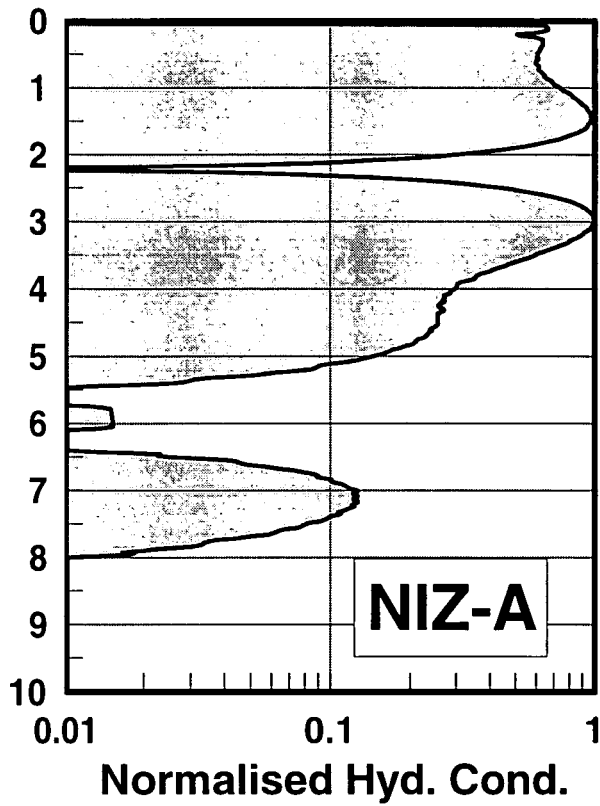


Figure 6.6. EK estimated, normalised hydraulic conductivity at 4 sites

